

Review

Combustion synthesis of refractory and hard materials: A review

Guanghua Liu ^{a,*}, Jiangtao Li ^{a,**}, Kexin Chen ^b^a Technical Institute of Physics and Chemistry, Key Laboratory of Functional Crystals and Laser Technology, Chinese Academy of Sciences, Beijing 100190, China^b Department of Materials Science and Engineering, State Key Laboratory of New Ceramics and Fine Processing, Tsinghua University, Beijing 100084, China

ARTICLE INFO

Article history:

Received 26 March 2012

Accepted 13 September 2012

Keywords:

Combustion synthesis

Refractory materials

Hard materials

Densification

Casting

Mechanical properties

ABSTRACT

Combustion synthesis is widely used for preparing various refractory and hard materials, including alloys, intermetallics, ceramics, and cermets. The unique reaction condition in combustion synthesis with extremely-high temperature and fast heating/cooling rate offers the products interesting microstructures and superior mechanical properties. In comparison with conventional powder metallurgy approaches, combustion synthesis exhibits the advantages of short processing time, less energy consumption, and lower cost, thus providing a more efficient way to produce refractory and hard materials.

This article reviews recent progress in combustion synthesis of refractory and hard materials, with an emphasis on the results reported in the last decade. Both the synthesis of powders and direct fabrication of bulk materials are discussed. For the synthesis of powders, results in two aspects are reviewed, viz. synthesis of ultrafine and especially nano-sized powders by thermal reduction reactions or post chemical etching, and synthesis of nitride and carbide powders in air. For direct fabrication of bulk materials, two techniques are involved, viz. combustion synthesis with simultaneous densification assisted by a mechanical or gas pressure, and combustion synthesis casting in a high-pressure Ar atmosphere or in a high-gravity field.

© 2012 Elsevier Ltd. All rights reserved.

Contents

1. Introduction	90
2. Combustion synthesis of refractory and hard powders	91
2.1. Combustion synthesis of ultrafine and especially nano-sized powders	91
2.2. Combustion synthesis of nitride and carbide powders in air	91
3. Combustion synthesis with simultaneous densification for preparing bulk refractory and hard materials	93
3.1. Combustion synthesis with simultaneous densification under a mechanical pressure	93
3.2. Combustion synthesis with simultaneous densification in a high-pressure N ₂ atmosphere	94
4. Combustion synthesis casting of bulk refractory and hard materials	96
4.1. Combustion synthesis casting in a high-pressure Ar atmosphere	96
4.2. Combustion synthesis casting in a high-gravity field	98
4.3. In-situ fabrication of metal matrix composites by incorporating combustion synthesis into conventional casting processes	100
5. Concluding remarks	100
Acknowledgments	100
References	100

1. Introduction

Combustion synthesis, which is also known as self-propagating high-temperature synthesis (SHS), is a method to produce inorganic

materials from exothermic combustion reactions. This method was discovered by Merzhanov and Borovinskaya [1] during their study on the phenomenon of solid flame. Since then, a great diversity of metal and ceramic materials has been prepared by combustion synthesis, and thousands of research papers have been published, covering all the aspects in this field from theoretical modeling to experimental investigation. Many review articles and book chapters have also been published [2–17], giving a more comprehensive overview of the progress of combustion synthesis in the past 40 years.

* Corresponding author.

** Corresponding author. Tel.: +86 10 82543693; fax: +86 10 82543695.

E-mail addresses: liugh02@mails.tsinghua.edu.cn (G. Liu), ljt0012@vip.sina.com (J. Li).

In contrast to conventional solid-state synthesis methods characterized by a longtime heat-treatment at high temperatures, combustion synthesis can be finished in a short time and requires much lower energy consumption, because it uses the heat energy released in combustion reactions and no furnace is necessary. With these merits, combustion synthesis offers an efficient way for industrial production of many inorganic materials. For example, many kinds of refractory and hard materials have been prepared by combustion synthesis, including alloys, intermetallics, ceramics, and cermets in a form of powders or consolidated bulks.

This article briefly reviews recent progress in combustion synthesis of refractory and hard materials, where both the synthesis of powders and direct fabrication of bulk materials are involved. For the synthesis of powders, the preparation of ultrafine and especially nano-sized powders was first discussed, and followed by the synthesis of nitride and carbide powders in air. For direct fabrication of bulk materials, two techniques are reviewed, which include combustion synthesis with simultaneous densification and combustion synthesis casting. Considering the large number of publications on the subject, the present review is mostly focused on the results reported in the last decade.

2. Combustion synthesis of refractory and hard powders

Combustion synthesis is widely used for preparing refractory and hard powders, and many carbide, nitride, boride, and oxynitride powders have been prepared by combustion synthesis [18–23]. In this aspect, results in two notable directions were reported in the last decade. One direction was the preparation of ultrafine and especially nano-sized powders, and the other was the synthesis of nitride and carbide powders in air, which are reviewed respectively as follows.

2.1. Combustion synthesis of ultrafine and especially nano-sized powders

For preparing bulk refractory and hard materials by sintering, the quality of the starting powders is of great concern. Compared with coarse powders, ultrafine powders with a submicron or even nano-scale particle size are favorable because of their larger specific surface area and higher sintering activity. Recent studies have shown that ultrafine powders can be produced by combustion synthesis from thermal reduction reactions or by post chemical etching [24–33].

Thermal reduction is an effective way to produce ultrafine refractory and hard powders. Nersisyan et al. prepared nano-sized WC powders by combustion synthesis from ($\text{WO}_3 + \text{NaN}_3 + \text{C}$) mixture with NaN_3 as a reducing agent [24]. The prepared WC powders showed an average grain size of 50–100 nm and the yield was about 25%. It was proposed that, the moderate reaction temperature (1000–1200 °C) and the presence of molten Na_2WO_4 suppressed the grain growth of WC and led to the formation of nanopowders. Ultrafine WC powders were also prepared by thermal reduction using Mg as the reducing agent [25–27], where alkali salts were added to promote mass transportation and facilitate the formation of single-phase WC product. By combustion synthesis from ($\text{WO}_3 + 3\text{Zn} + 4\text{NaCl}$), nano-sized W powders with a batch of 12 kg were prepared [28]. The oxygen concentration in the W powders could be reduced to 0.3 wt.% by post annealing in a flowing H_2 atmosphere. In a similar way, Jiang et al. prepared submicron W powders by combustion synthesis using Na_2WO_4 instead of WO_3 as the W-source [29]. This can provide a more economic approach to produce W powders because Na_2WO_4 is cheaper than WO_3 . Following the thermal reduction method, Jiang et al. also prepared submicron B_4C powders by combustion synthesis from ($\text{Na}_2\text{B}_4\text{O}_7 + \text{Mg} + \text{C}$) [30]. In contrast to B_2O_3 , which is readily converted into H_3BO_3 by the absorption of moisture in air, $\text{Na}_2\text{B}_4\text{O}_7$ is a stable B-source.

Besides thermal reduction, combustion synthesis with post chemical etching is an effective way for preparing ultrafine powders. Combustion synthesis is a complex process, where chemical reactions are

accompanied by structure formation. For some reaction systems, the primary product particles have a size of 0.1–0.2 μm , as revealed by quenching experiments [31]. During combustion reactions, the primary particles often agglomerate and form larger blocks, which are usually observed in the products. The agglomeration of the primary particles can be destroyed by chemical etching. By combustion synthesis with post chemical etching, Borovinskaya et al. prepared a variety of refractory nanopowders [32]. It was found that, successive chemical etching and dispersing of raw products led to a decrease in particle size by the dissolution and washout of impurities and intermediate products. As an example, nano-sized MoSi_2 powders were produced by combustion synthesis, and the $\text{SiO}_2\text{--MoO}_3$ oxide layer at the surface of MoSi_2 particles was removed by hot alkali etching [33].

Nano-sized refractory and hard powders can also be produced by N_2 -catalytic combustion reactions. Liu et al. reported combustion synthesis of nano-sized $\beta\text{-SiC}$ powders in a N_2 atmosphere with Si and carbon black as reactants [34]. The average grain size of the $\beta\text{-SiC}$ powders was readily below 100 nm (Fig. 1). Based on the experimental results and thermodynamic calculation, it was proposed that combustion synthesis of SiC in N_2 included two steps: (1) Si reacted with N_2 to form Si_3N_4 ; (2) the initially-formed Si_3N_4 decomposed at higher temperatures and the released Si reacted with carbon black to produce SiC. In the synthesis process, N_2 joined the reaction at first but was released later, and finally the net consumption of N_2 was zero. That is to say, N_2 played a role of catalyst in the synthesis of SiC.

From the above results, combustion synthesis is effective in preparing ultrafine powders of refractory and hard materials. Compared with most conventional methods for preparing ultrafine powders, combustion synthesis exhibits a short reaction time, lower energy consumption, and the availability for mass production. To produce ultrafine powders with a higher purity and homogeneity by combustion synthesis, proper post-treatments of the raw products are often required.

2.2. Combustion synthesis of nitride and carbide powders in air

In the family of refractory and hard materials, nitrides and carbides are two important members. Combustion synthesis of nitride and carbide powders was usually carried out in N_2 or Ar atmosphere. In 1994, Tsuchida et al. reported the formation of AlN after combustion of ($\text{Al} + \text{C}$) powder mixture in air [35]. Similar phenomena were observed later in other powders such as La, ($\text{Al} + \text{Zr-Al alloy}$), Al, and Ti, where nitrides were obtained as the major products after the combustion of metallic powders in air [36–38]. Liu et al. investigated the combustion of Ti powders in air and found that different products were synthesized in different parts of the sample [39]. TiO_2 was found at the top surface of the sample, TiN was obtained as the major product in upper and center parts, and much un-reacted Ti remained at the bottom (Fig. 2). It was proposed that, the formation of TiN was fulfilled by a

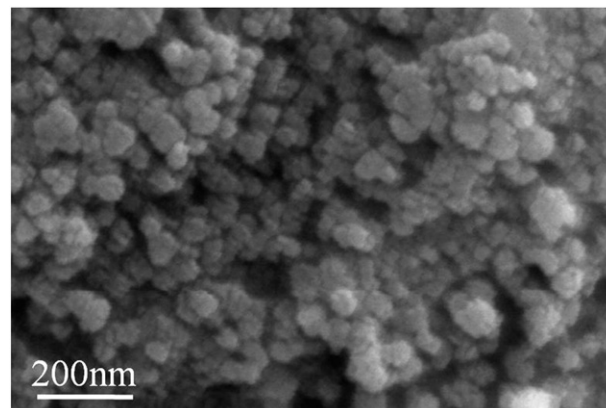


Fig. 1. SEM image of nano-sized $\beta\text{-SiC}$ powders prepared by combustion synthesis in N_2 .

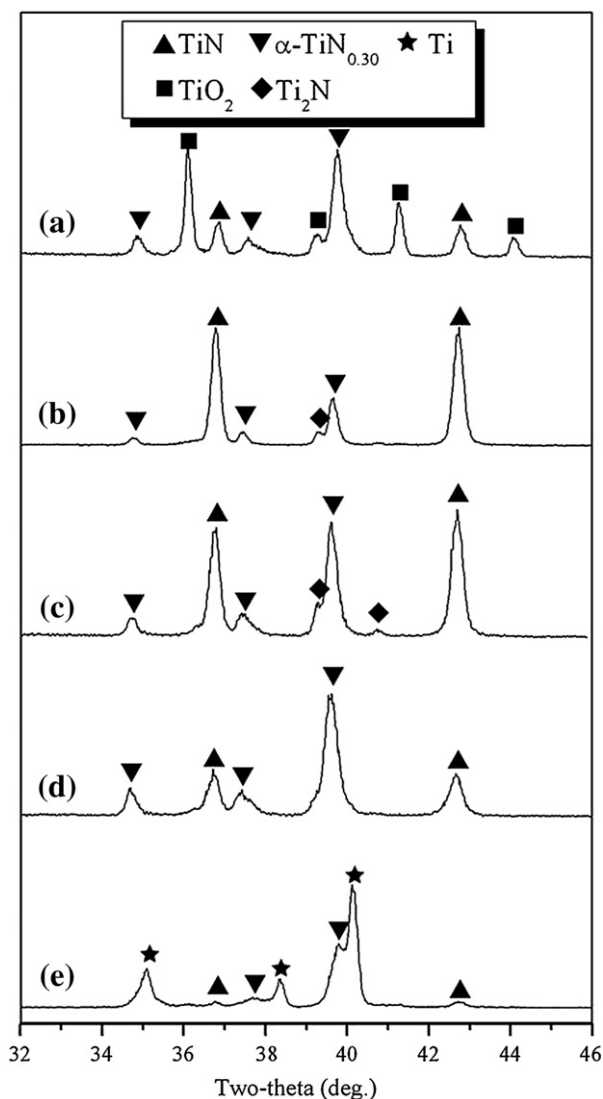


Fig. 2. XRD patterns of the products obtained in different parts of the sample after combustion of Ti powders in air: (a) top surface; (b) upper part; (c) center part; (d) lower part; (e) bottom [39].

kinetically-controlled reaction process, where the infiltration of N_2 and O_2 gases played an important role. In this process, the combustion reaction started with the oxidation of Ti, and O_2 was almost depleted at the top surface of the sample. Because the gas infiltration was slower than the propagation of combustion wave, the concentration of O_2 was very low in the center part of the sample, and consequently nitrides were produced. By adding some NH_4Cl or carbon black in the Ti powder compacts, the gas infiltration could be enhanced and the content of un-reacted Ti was reduced.

Mei and Li reported the synthesis of AlN–SiC solid solution by combustion of $(Al + C + Si_3N_4)$ powders in air [40]. They proposed that the selective reaction of Al with N_2 instead of O_2 was caused by the difference in infiltration rates of the two gases, where the infiltration flux ratio of N_2/O_2 was calculated to be 6.99. The selective reaction mechanism was later applied in combustion synthesis of Si_3N_4 powders in air [41]. After the combustion of Si powders in air, both Si_3N_4 and minor Si_2N_2O were produced at the sample's surface, and in the interior part of the sample only Si_3N_4 was obtained, as confirmed by FTIR and XRF analysis (Fig. 3). From XRF results, the oxygen content in the product obtained in the interior part was below 5 wt.%. In addition to AlN and Si_3N_4 , α -SiAlON was prepared by combustion synthesis in air [42]. In contrast to the pure nitrides, α -SiAlON is an

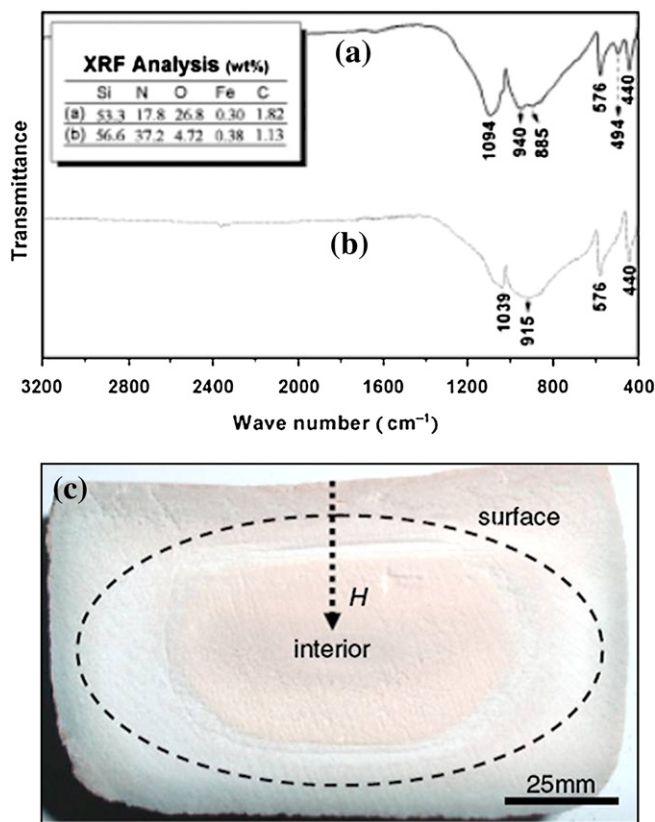


Fig. 3. FTIR spectra and XRF results of the products obtained at (a) surface and (b) interior part of the sample after combustion of Si powders in air, with a photograph of the sample shown in (c) [41].

oxynitride compound that can incorporate O atoms into its lattice. In this way, a higher yield can be realized for α -SiAlON than pure nitrides by combustion synthesis in air. Combustion synthesis in air was also used to prepare carbide powders. For example, ultrafine β -SiC powder was synthesized by combustion of $(Si + C)$ powder mixture in air [43]. It was found that the combustion reaction occurred in a two-stage mode. In the first stage, the flame showed a red color with a maximum temperature of nearly 800 °C. In the second stage, bright flame was observed and the maximum temperature reached about 1750 °C. It was proposed that the formation of SiC was mostly finished in the second stage.

For combustion synthesis in air under lower pressures of N_2 and O_2 , a higher reactivity of reactant powders is necessary to realize a stable self-propagating combustion reaction. To improve the reactivity of reactant powders, mechanical activation is often used, where high-energy milling is applied to reduce the particle size and create more fresh surfaces, and intensive mechanical activation can induce self-ignition in some cases. Liu et al. reported the self-ignition and sustained combustion of mechanically-activated $(Ti + Al + C)$ powder mixture in air [44]. In the combustion product, hollow near-spherical Ti–Al–C agglomerates were observed with a two-layered shell structure. The outer layer was composed of lamellar Ti–Al–C ternary phases, and the inner layer consisted of equiaxed TiC grains (Fig. 4). It was proposed that the occurrence of a Ti–Al melt was important to the formation of the hollow agglomerates.

In comparison with the methods to synthesize nitride and carbide powders in a high-pressure N_2 or Ar atmosphere, combustion synthesis in air requires much simpler equipment and offers larger batch size, which is attractive for large-scale production of nitride and carbide powders with lower costs. The major drawback of this method is the existence of oxide impurities in the products, and thus further investigations are necessary to improve the purity of the products.

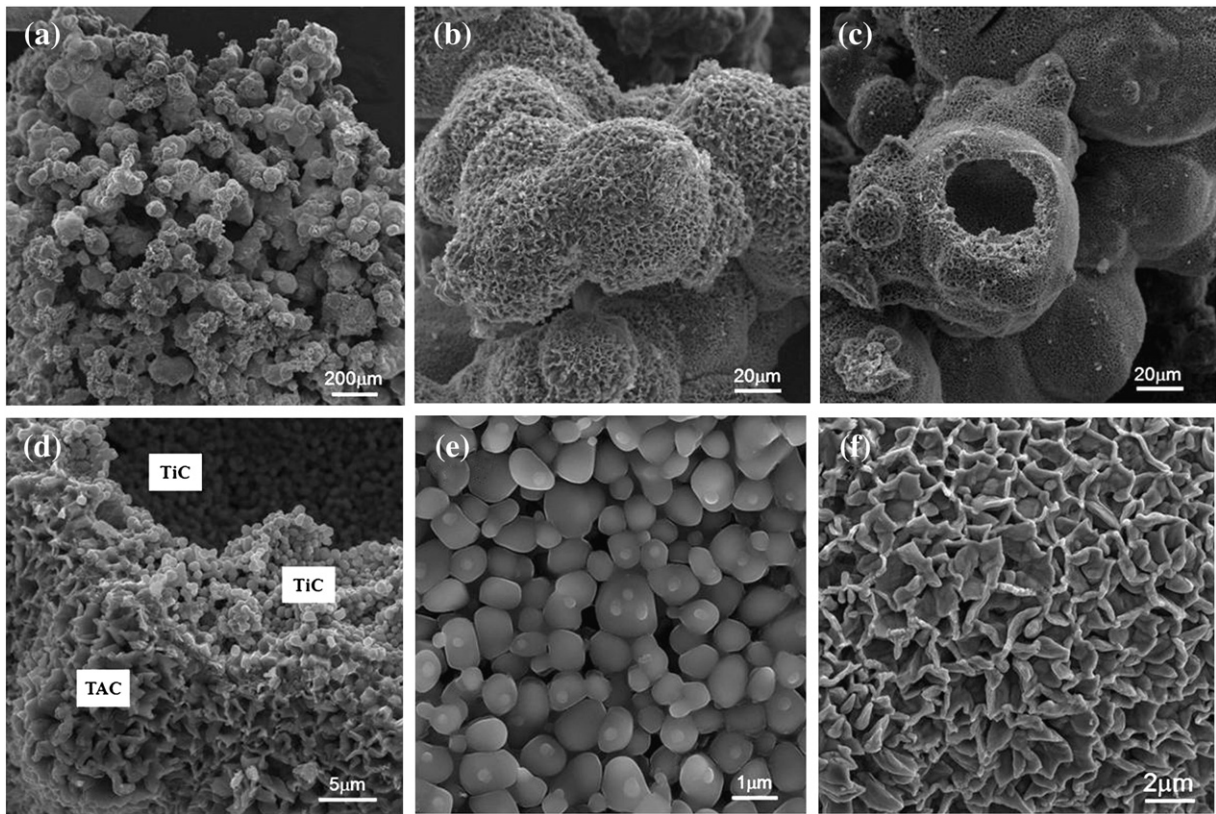


Fig. 4. SEM images of the hollow near-spherical Ti–Al–C agglomerates: (a) and (b) overviews of the agglomerates; (c) and (d) walls of an agglomerate; (e) equiaxed TiC grains; (f) lamellar Ti–Al–C ternary phases [44].

3. Combustion synthesis with simultaneous densification for preparing bulk refractory and hard materials

In addition to the production of powders, direct fabrication of bulk refractory and hard materials can be realized by combustion synthesis when it is combined with simultaneous densification. The simultaneous densification can be carried out in different ways, such as uniaxial hot-pressing, pseudo hot isostatic pressing, spark plasma sintering, and extrusion, where samples are consolidated under a mechanical pressure. Gas pressure can also be applied for simultaneous densification, and as examples several refractory and hard ceramic composites have been prepared by combustion synthesis in a high-pressure N_2 atmosphere.

3.1. Combustion synthesis with simultaneous densification under a mechanical pressure

Early investigations on the fabrication of bulk materials by combustion synthesis with simultaneous densification can be found nearly 30 years ago [45]. In the last decade, many new results on this topic were reported, with more approaches for simultaneous densification developed and a large diversity of refractory and hard materials explored [46–75].

Shon et al. prepared lots of consolidated intermetallics and cermets by combustion synthesis with simultaneous densification by uniaxial hot-pressing [50–58]. The prepared NiAl and Ni_3Al bulk intermetallics showed a high relative density of 99.8% [53]. Consolidated WC and WC–Co materials with a submicron grain size were also fabricated, showing a hardness of 27.08 GPa and a fracture toughness of $15.1 \text{ MPa} \cdot \text{m}^{1/2}$ [54,55]. Recently, they used combustion synthesis with simultaneous densification to prepare nanostructured composites of intermetallics and ceramics [59–63]. As an example, WSi_2 –SiC composite was fabricated with a relative density of 99.8%. In the composite, the average grain sizes of WSi_2 and SiC were 47

and 38 nm, respectively. Owing to the nano-scale microstructure, the WSi_2 –SiC composite exhibited a hardness of 16.98 GPa and a fracture toughness of $4.8 \text{ MPa} \cdot \text{m}^{1/2}$ [63].

Zhang et al. reported combustion synthesis with simultaneous densification by pseudo hot isostatic pressing, and prepared several ceramic composites and cermets [64–69]. The prepared TiC– TiB_2 ceramic composite showed a relative density of 96.8%, and its hardness and compressive strength reached 93 HRA and 2.68 GPa [64]. The prepared cermets, such as TiC–Ni, TiC–Fe, TiB–Ti, and TiB_2 –Cu, exhibited a homogeneous microstructure with ceramic particles uniformly dispersed in the metals. In the TiC–Fe cermet, the particle size of TiC decreased with increasing content of Fe (Fig. 5) [66].

Combustion synthesis coupled with spark plasma sintering is another method to realize simultaneous densification. Using this method, Wang et al. prepared some cermets and ceramic composites such as Ti_5Si_3 /TiC, Ti_3SiC_2 –SiC, and ZrB_2 –SiC [70–73]. The Ti_3SiC_2 –SiC composites contained nano-sized SiC particles and showed a flexural strength of $501 \pm 50 \text{ MPa}$ [71]. For the ZrB_2 –SiC composites, the relative density reached 98.5%, and the hardness and fracture toughness were $17.18 \pm 0.26 \text{ GPa}$ and $4.31 \pm 0.20 \text{ MPa} \cdot \text{m}^{1/2}$, respectively [72].

Simultaneous densification can also be fulfilled by combining combustion synthesis with extrusion. Morsi et al. studied the reactive extrusion of Ni_3Al intermetallics, where the extruded sample showed a much lower porosity ($<0.5\%$) and smaller grain size ($4.5 \pm 2.2 \mu\text{m}$) than that without extruding, which had a porosity of 18% and a grain size of $28.4 \pm 1.7 \mu\text{m}$. The reduction in porosity and grain size offered the extruded sample an increase in hardness by nearly 40% [74]. Equal channel angular extrusion followed by combustion synthesis of Ti–Al intermetallics was also investigated, revealing that a higher number of passes led to a lower porosity and more homogeneous microstructure in the product [75].

The consolidated bulk materials prepared by combustion synthesis with simultaneous densification exhibited good mechanical properties.

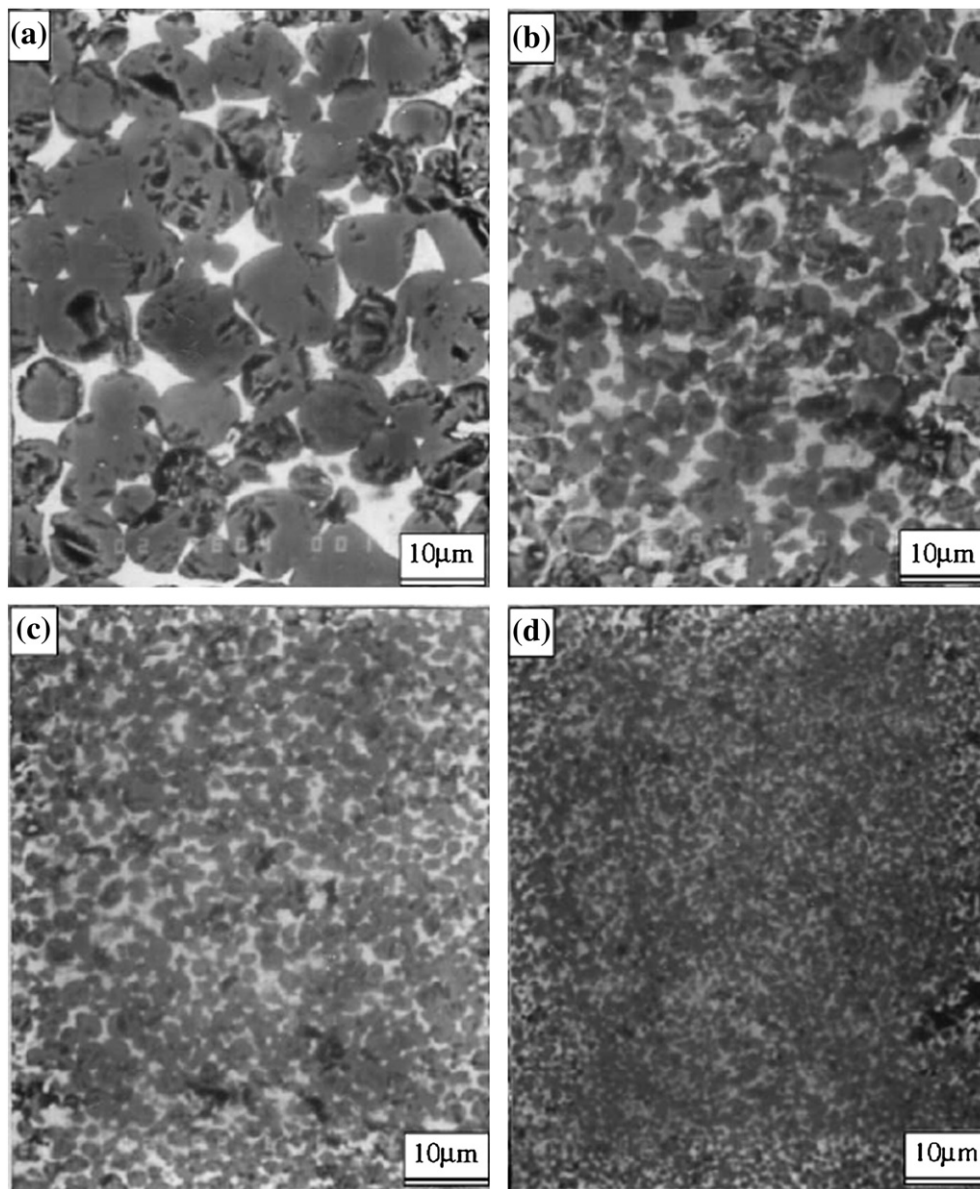


Fig. 5. SEM images of TiC–Fe cermets prepared by combustion synthesis with pseudo hot isostatic pressing: (a) 10 wt.% Fe; (b) 20 wt.% Fe; (c) 30 wt.% Fe; (d) 40 wt.% Fe [66].

Shu et al. investigated the compressive properties and wear resistance of some combustion-synthesized cermets [76–79]. It was found that, the compressive strength, ductility, work-hardening capacity of TiC_x/Al cermets were greatly enhanced by adding Mg, Zn, and Sn, respectively (Fig. 6) [76]. The mechanical properties of TiC_x/Al composites also depended on the volume fraction of TiC_x particles, and with increasing volume fraction of TiC_x , the yield strength, hardness, and wear resistance were all improved [77]. Similar result was observed in NiAl-based composites reinforced by ceramic particles, where the compressive strength increased with increasing content of ceramic particles and reached 1497 MPa with 5 wt.% ceramic particles [79]. More refractory and hard materials prepared by combustion synthesis with simultaneous densification and their properties are summarized in Table 1.

By combustion synthesis with simultaneous densification under a mechanical pressure, bulk refractory and hard materials can be rapidly fabricated. In contrast to the powder metallurgy approaches, combustion synthesis with simultaneous densification does not require external heating sources and is a furnace-free method. Using this method to prepare bulk materials, however, a careful control of the whole processing is necessary to obtain highly-dense samples with

uniform microstructures, which includes the selection of reaction systems, proper design of dies, and determination of the time to exert the pressure.

3.2. Combustion synthesis with simultaneous densification in a high-pressure N_2 atmosphere

Simultaneous densification can be realized by combustion synthesis in a high-pressure N_2 atmosphere. Shibuya et al. reported combustion synthesis of TiN– TiB_2 ceramic composites from (Ti + BN) in a N_2 atmosphere with a pressure of <10 MPa [80]. They found that the hardness of the composites increased with increasing N_2 pressure and showed a maximum of 25 GPa. Consolidated TiN– TiB_2 composite with both high hardness and good fracture toughness was obtained under a N_2 pressure of 4 MPa. For the samples produced under a N_2 pressure of >6 MPa, macro-cracks were observed due to thermal shock. Smirnov et al. prepared β -SiAlON-based ceramic composites by combustion synthesis under a N_2 pressure of 100 MPa [81,82]. The relative density of the composites depended on the kind and content of secondary phases, and reached the maximum of 94–96%. For

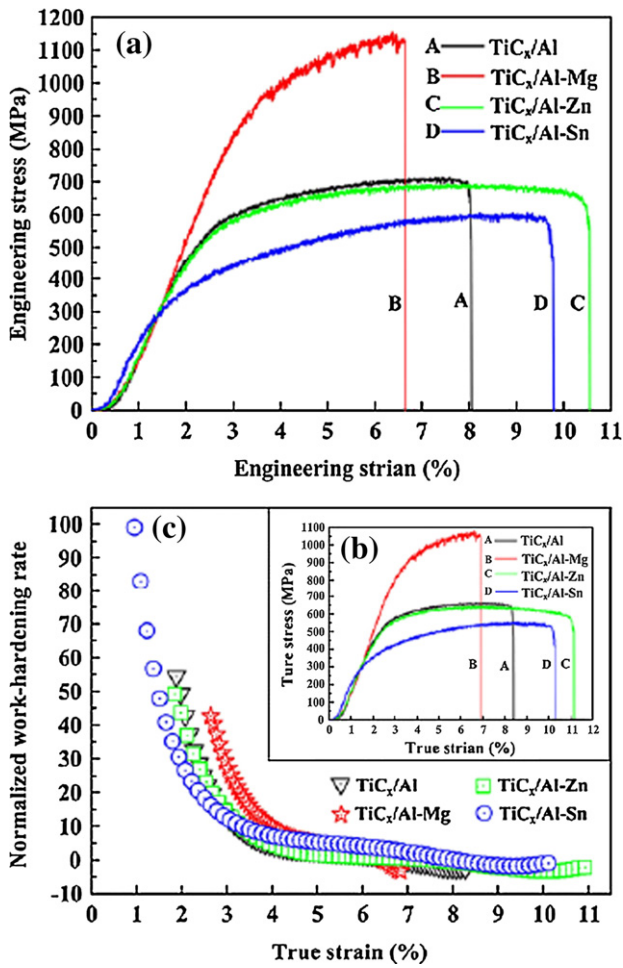


Fig. 6. Compressive properties of TiC_x/Al composites with the alloy elements (Mg, Zn, Sn): (a) engineering stress-strain curves; (b) true stress-strain curves; (c) normalized work-hardening rate vs. true strain [76].

β -SiAlON-BN composites, the relative density, friction coefficient, and wear resistance all decreased with increasing BN content.

Li et al. reported combustion synthesis of AlN-TiN-BN-SiC ceramic composites from $(\text{B}_4\text{C} + \text{Si} + \text{Al} + \text{TiN})$ under a N_2 pressure of 100 MPa [83]. It was found that, the microstructure, mechanical properties, and thermal shock resistance of the composites were strongly affected by the volume fraction of $(\text{AlN} + \text{TiN})$. A higher volume fraction of $(\text{AlN} + \text{TiN})$ led to an increased relative density and better mechanical properties (Fig. 7), and the maximum relative density of 95.5% was observed with 70 vol.% $(\text{AlN} + \text{TiN})$. With increasing volume fraction of $(\text{AlN} + \text{TiN})$, the grain sizes of AlN and BN decreased, and the fracture behavior of the composites transformed from intergranular to transgranular mode. The AlN-TiN-BN-SiC composites showed good thermal shock resistance, with no evident decrease for a thermal shock temperature of $<600^\circ\text{C}$. Water quenching experiments revealed that, for the composites with 30, 50, and 70 vol.% $(\text{AlN} + \text{TiN})$, the critical temperatures for retaining 70% of the initial strength were 1200, 850, and 670°C , respectively. By combustion synthesis in a high-pressure N_2 atmosphere, BN-Ti(C,N) ceramic composites were also prepared, where a higher Ti(C,N) content resulted in better mechanical properties [84].

Combustion synthesis in a high-pressure N_2 atmosphere is another method to realize simultaneous densification and prepare nitride-based refractory and hard materials. In this method, gas pressure instead of usually-used mechanical pressure is applied to assist the densification. A technical problem with this method is the extremely-high N_2 pressure

Table 1

Examples of refractory and hard materials prepared by combustion-synthesis-based methods and their properties.

Materials	Methods	Properties	Ref.
$\text{TiC-Cr}_3\text{C}_2$	CS + HP $P = 30 \text{ MPa}$		[46]
$\text{MgAl}_2\text{O}_4\text{-TiAl}$	CS + HP $P = 80 \text{ MPa}$	$\text{RD} \geq 98\%$	[47]
$\text{Al}_2\text{O}_3\text{-TiAl/Ti}_3\text{Al}$	CS + HP $P = 50 \text{ MPa}$	$\text{RD} = 98\%$	[48]
TiSi_3C_2 -based composites	CS + HP $P = 80 \text{ MPa}$	$\text{RD} = 95\%$	[49]
$\text{NiAl, Ni}_3\text{Al}$	CS + HP $P = 275 \text{ MPa}$	$\text{RD} = 99.8\%$ $H = 2.8\text{--}3.5 \text{ GPa}$	[53]
MoSi_2	CS + HP $P = 60 \text{ MPa}$	$\text{RD} = 98\%$ $H = 10.5 \text{ GPa}$, $K_{\text{IC}} = 3.5 \text{ MPa}\cdot\text{m}^{1/2}$	[54]
WC, WC-Co	CS + HP $P = 60 \text{ MPa}$	$\text{RD} = 70\%$ for WC, $\text{RD} = 98.5\%$ for WC-5vol.%Co $H = 19.28 \text{ GPa}$, $K_{\text{IC}} = 15.1 \text{ MPa}\cdot\text{m}^{1/2}$	[55]
$\text{MoSi}_2\text{-SiC}$	CS + HP $P = 60 \text{ MPa}$	$\text{RD} = 98\%$, $d(\text{MoSi}_2) = 3.5 \mu\text{m}$, $d(\text{SiC}) = 1.5 \mu\text{m}$ $H = 14.1 \text{ GPa}$, $K_{\text{IC}} = 4.8 \text{ MPa}\cdot\text{m}^{1/2}$	[56]
WC	CS + HP $P = 60 \text{ MPa}$	$\text{RD} = 98.5\%$, $d = 0.43\text{--}0.6 \mu\text{m}$ $H = 25.52\text{--}27.08 \text{ GPa}$, $K_{\text{IC}} = 4.4\text{--}4.8 \text{ MPa}\cdot\text{m}^{1/2}$	[57]
NbSi_2	CS + HP $P = 60 \text{ MPa}$	$\text{RD} = 98\%$, $d = 0.3 \mu\text{m}$ $H = 8.76 \text{ GPa}$, $K_{\text{IC}} = 2.5 \text{ MPa}\cdot\text{m}^{1/2}$	[58]
$\text{ZrSi}_2\text{-Si}_3\text{N}_4$	CS + HP $P = 60 \text{ MPa}$	$\text{RD} = 98\%$, $d(\text{ZrSi}_2) = 84 \text{ nm}$, $d(\text{Si}_3\text{N}_4) = 59 \text{ nm}$ $H = 7.55 \text{ GPa}$, $K_{\text{IC}} = 4.6 \text{ MPa}\cdot\text{m}^{1/2}$	[59]
$\text{NbSi}_2\text{-Si}_3\text{N}_4$	CS + HP $P = 60 \text{ MPa}$	$\text{RD} = 98\%$ $H = 7 \text{ GPa}$, $K_{\text{IC}} = 3.5 \text{ MPa}\cdot\text{m}^{1/2}$	[60]
$\text{TaSi}_2\text{-SiC-Si}_3\text{N}_4$	CS + HP $P = 60 \text{ MPa}$	$\text{RD} = 96\%$, $d = 35\text{--}72 \text{ nm}$ $H = 12.50 \text{ GPa}$, $K_{\text{IC}} = 4 \text{ MPa}\cdot\text{m}^{1/2}$	[61]
$\text{ZrSi}_2\text{-SiC}$	CS + HP $P = 60 \text{ MPa}$	$\text{RD} = 97\%$, $d(\text{ZrSi}_2) = 170 \text{ nm}$, $d(\text{SiC}) = 90 \text{ nm}$ $H = 12.06 \text{ GPa}$, $K_{\text{IC}} = 3 \text{ MPa}\cdot\text{m}^{1/2}$	[62]
$\text{WSi}_2\text{-SiC}$	CS + HP $P = 80 \text{ MPa}$	$\text{RD} = 99.8\%$, $d(\text{WSi}_2) = 47 \text{ nm}$, $d(\text{SiC}) = 38 \text{ nm}$ $H = 16.98 \text{ GPa}$, $K_{\text{IC}} = 4.8 \text{ MPa}\cdot\text{m}^{1/2}$	[63]
TiC-TiB_2	CS + PHIP $P = 160 \text{ MPa}$	$\text{RD} = 90.5\text{--}96.8\%$ $H = 85.5\text{--}63.5 \text{ HRA}$, $K_{\text{IC}} = 3.5\text{--}5.8 \text{ MPa}\cdot\text{m}^{1/2}$ $\sigma_b = 405\text{--}450 \text{ MPa}$, $\sigma_c = 1.97\text{--}2.68 \text{ GPa}$	[64]
$\text{TiC-(20-50)wt.\%Ni}$	CS + PHIP	$\text{RD} = 94.3\text{--}96.8\%$ $H = 84.3\text{--}88.5 \text{ HRA}$, $\sigma_b = 876\text{--}1116 \text{ MPa}$	[65]
$\text{TiB-(20-60)wt.\%Ti}$	CS + PHIP $P = 160 \text{ MPa}$	$\text{RD} = 94.3\text{--}98.5\%$ $H = 82.7\text{--}87.8 \text{ HRA}$, $K_{\text{IC}} = 5.2\text{--}6.2 \text{ MPa}\cdot\text{m}^{1/2}$ $\sigma_b = 193\text{--}515 \text{ MPa}$, $\sigma_c = 1.74\text{--}2.41 \text{ GPa}$ $\sigma_t = 140\text{--}280 \text{ MPa}$	[67]
$\text{TiB}_2\text{-40wt.\%Cu}$	CS + PHIP	$\text{RD} = 96.1\%$ $H = 76.5 \text{ HRA}$, $K_{\text{IC}} = 8.3 \text{ MPa}\cdot\text{m}^{1/2}$, $\sigma_b = 583 \text{ MPa}$	[68]
Cu-30wt.\%TiB_2	CS + PHIP	$H = 48 \text{ HRC}$, $K_{\text{IC}} = 10.4 \text{ MPa}\cdot\text{m}^{1/2}$, $\sigma_y = 312 \text{ MPa}$	[69]
$\text{Ti}_3\text{SiC}_2\text{-SiC}$	CS + SPS	$\text{RD} > 98\%$, $d(\text{Ti}_3\text{SiC}_2) = 5 \mu\text{m}$, $d(\text{SiC}) = 0.1 \mu\text{m}$ $H = 9.2 \text{ GPa}$, $\sigma_b = 501 \pm 50 \text{ MPa}$	[71]
$\text{ZrB}_2\text{-SiC}$	CS + SPS	$\text{RD} = 98.5\%$, $d(\text{ZrB}_2) < 5 \mu\text{m}$, $d(\text{SiC}) < 1 \mu\text{m}$ $H = 17.18 \pm 0.26 \text{ GPa}$, $K_{\text{IC}} = 4.31 \pm 0.20 \text{ MPa}\cdot\text{m}^{1/2}$	[72]
$\text{ZrB}_2\text{-SiC}$	CS + SPS	$\text{RD} = 86.4\text{--}98.3\%$ $H = 10.8\text{--}18.6 \text{ GPa}$, $K_{\text{IC}} = 3.6\text{--}5.3 \text{ MPa}\cdot\text{m}^{1/2}$	[73]
TiC-Al	CS + HP $P = 64 \text{ MPa}$	$\sigma_c = 557\text{--}1028 \text{ MPa}$, $H_c = 0.42\text{--}2.04$	[76]
TiC-Al	CS + HP	$H = 2.17\text{--}2.54 \text{ GPa}$, $\sigma_c = 714\text{--}815 \text{ MPa}$	[77]
$\text{Ti}_2\text{AlC-TiAl}$	CS + HP $P = 16 \text{ MPa}$	$\sigma_c = 1301\text{--}1649 \text{ MPa}$, $H_c = 0.89\text{--}1.25$	[78]
$\text{NiAl-based composites}$	CS + HP	$\sigma_c = 1497\text{--}1879 \text{ MPa}$, $H_c = 0.91\text{--}1.29$	[79]

(continued on next page)

Table 1 (continued)

Materials	Methods	Properties	Ref.
TiN–TiB ₂	CS in N ₂ P = 4 MPa	RD > 90%, $H = 25$ GPa, $K_{IC} = 5.9$ MPa·m ^{1/2}	[80]
SiAlON-based composites	CS in N ₂ P = 100 MPa	RD = 72–96%	[81,82]
AlN–TiN–BN–SiC	CS in N ₂ P = 100 MPa	RD = 85.3–95.5% $H = 0.17$ – 1.18 GPa, $K_{IC} = 1.7$ – 5.0 MPa·m ^{1/2} $\sigma_b = 60$ – 260 MPa	[83]
BN–Ti(C,N)	CS in N ₂ P = 100 MPa	$H = 0.15$ – 0.45 GPa, $K_{IC} = 0.7$ – 1.1 MPa·m ^{1/2} $\sigma_b = 42.3$ – 67.1 MPa	[84]
Fe–B alloy	CS in Ar P = 7 MPa	$\sigma_c = 1710$ MPa, $\alpha_y = 1430$ MPa, $\epsilon_f = 19.8\%$	[88]
Cu ₆₀ Fe ₄₀ alloy	CS in Ar P = 8 MPa	$\sigma_c = 1050$ MPa, $\alpha_y = 540$ MPa, $\epsilon_f = 20.9\%$	[93]
Ni ₆₅ Al ₂₁ Cr ₁₄ alloy	CS in Ar P = 4 MPa	$\sigma_c = 2200$ MPa, $\epsilon_f = 26\%$	[94]
Fe ₃ Al	CS in Ar P = 5 MPa	RD = 98% $\sigma_b = 1170$ MPa, $\alpha_y = 1050$ MPa	[95]
MoSi ₂ –(10–20) wt.%SiC	CS in Ar P = 5 MPa	$H = 8.4$ – 9.8 GPa, $K_{IC} = 3.3$ – 5.2 MPa·m ^{1/2}	[96]
Al ₂ O ₃ –ZrO ₂ (Y ₂ O ₃)	HGCS	RD = 98.6–99.8% $H = 22.1$ – 22.8 GPa, $K_{IC} = 12.6$ – 14.8 MPa·m ^{1/2} $\sigma_b = 1268$ – 1568 MPa	[97–99]
Al ₂ O ₃ –ZrO ₂ (Y ₂ O ₃)	HGCS	RD = 99.8% $H = 15.4$ – 15.7 GPa, $K_{IC} = 16.5$ – 17.9 MPa·m ^{1/2}	[100]
Al ₂ O ₃ –Y ₃ Al ₅ O ₁₂ – ZrO ₂	HGCS	RD = 99.3% $H = 17.8$ GPa, $K_{IC} = 5.5$ MPa·m ^{1/2}	[101]
TiC–TiB ₂	HGCS	RD = 99.2% $H = 28.5$ GPa, $K_{IC} = 6.2 \pm 0.5$ MPa·m ^{1/2} , $\sigma_b = 750 \pm 25$ MPa	[103]
Y–Al–Si–O glass	HGCS	$H = 7.9$ – 8.6 GPa	[111]
FeNiCr–TiC	HGCS	$H = 62.6$ HRC	[117]
AZ91(Mg alloy)– TiC	CS + Casting	$H = 83$ HB, $\sigma_t = 214$ MPa, $\epsilon_f = 4\%$	[119]
Steel–TiC	CS + Casting	$H = 57$ HRC	[121]
Steel–TiC/TiB ₂	CS + Casting	$H = 42.7$ – 47.1 HRC	[125]

Abbreviations in Table 1:

CS: combustion synthesis, HP: hot-pressing, P: pressure, PHIP: pseudo hot isostatic pressing, SPS: spark plasma sintering, HGCS: high-gravity combustion synthesis. RD: relative density, d : grain size, H : hardness, K_{IC} : fracture toughness, σ_b : bending or flexural strength, σ_c : compressive strength, σ_t : tensile strength, α_y : yield strength, H_c : work-hardening capacity, ϵ_f : fracture strain.

(e.g. 100 MPa) and thus complicated equipment, which can limit its application for industrial production.

4. Combustion synthesis casting of bulk refractory and hard materials

In combustion synthesis, if the reaction temperature exceeds the melting point of the products, it is possible to prepare consolidated bulk materials by melt casting. In contrast to conventional casting processes, combustion synthesis casting is a furnace-free technique with lower energy consumption. To prepare bulk refractory and hard materials by combustion synthesis casting, strongly-exothermic aluminothermic reactions are usually used to realize a high temperature. In aluminothermic reactions, two molten phases will be produced, viz. a metallic melt and an Al₂O₃-based ceramic melt. By controlling the separation degree of the two phases, various materials can be produced, including metals, ceramics, and cermets.

In the last decade, two techniques of combustion synthesis casting were developed: (1) combustion synthesis casting in a high-pressure Ar atmosphere, mostly used for preparing alloys; (2) combustion synthesis casting in a high-gravity field, mostly used for preparing ceramics. By the two techniques, a large variety of consolidated refractory and hard materials has been produced, which is reviewed as follows.

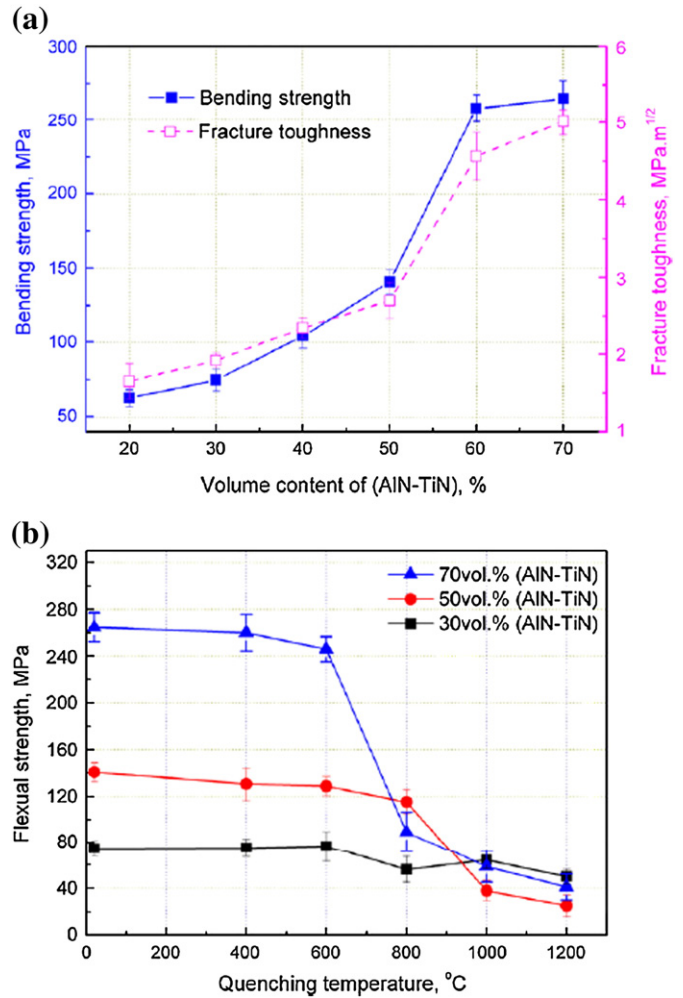


Fig. 7. Mechanical properties and thermal shock resistance of AlN–TiN–BN–SiC ceramic composites prepared by combustion synthesis under a N₂ pressure of 100 MPa: (a) bending strength and fracture toughness depending on the (AlN–TiN) content; (b) residual strength as a function of thermal shock temperature [83].

4.1. Combustion synthesis casting in a high-pressure Ar atmosphere

By combustion synthesis casting from aluminothermic reactions (e.g. $2Al + Fe_2O_3 = 2Fe + Al_2O_3$, $2Al + 3CuO = 3Cu + Al_2O_3$) in a high-pressure Ar atmosphere, Yang et al. prepared a large diversity of bulk alloys [85–94], including Fe-based alloys, Cu-based alloys, and other alloys. Owing to the fast cooling and solidification in combustion synthesis melting, unique microstructures such as nanograins, quasicrystals, and amorphous structure were produced in the prepared alloys and offered the alloys interesting properties.

Fe–B alloy with a nanostructured hypoeutectic microstructure was fabricated by combustion synthesis casting in an Ar atmosphere with a pressure of 7 MPa [88]. The microstructure of the alloy was characterized by a lamellar eutectic with α -Fe and t-Fe₂B, with an interphase spacing of ~50 nm and eutectic colony size of 3–25 μ m. In compressive tests, the Fe–B alloy showed a high yield strength of 1430 MPa and a large ductility of 19.8%. Fe₇₄Si₂₄B₂ alloy with the dimension of $\Phi 50$ mm \times 5 mm was also prepared, as shown in Fig. 8 [90]. The alloy consisted of (Fe₂B + Fe₃Si) eutectic and Fe₃Si matrix with an average grain size of ~10 nm. It was proposed that, the applied Ar pressure favored the formation of nano-crystallites by increasing the nucleation rate of Fe₃Si and slowing down the atomic diffusion in the super-cooling melt. Similar nano-scaled microstructure was observed in Cu₆₀Fe₄₀ alloy prepared by combustion synthesis casting

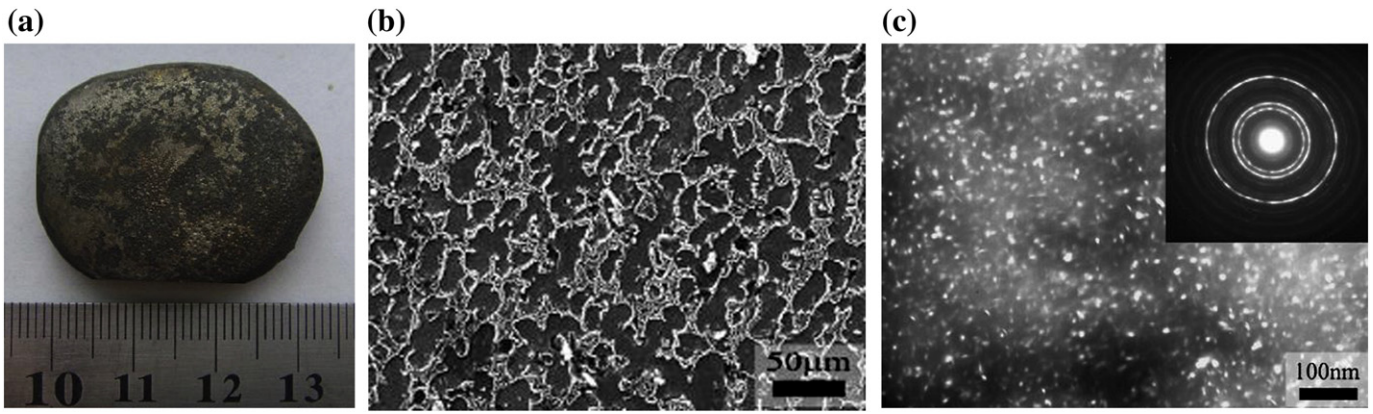


Fig. 8. $\text{Fe}_{74}\text{Si}_{24}\text{B}_2$ alloy prepared by combustion synthesis casting in an Ar atmosphere of 8 MPa: (a) photograph; (b) SEM image; (c) TEM image with SAED pattern [90].

from the reaction of $3\text{CuO} + 2\text{Al} + 2\text{Fe} = 1/20\text{Cu}_{60}\text{Fe}_{40} + \text{Al}_2\text{O}_3$ [93]. In the $\text{Cu}_{60}\text{Fe}_{40}$ alloy, coarse dendrites were embedded in the matrix with a grain size of 50–300 nm, and no compositional separation was observed. The yield strength of the $\text{Cu}_{60}\text{Fe}_{40}$ alloy reached 540 MPa and was clearly higher than that of commercial Cu–Fe alloys. Nanostructured $\text{Ni}_{65}\text{Al}_{21}\text{Cr}_{14}$ alloy with the dimension of $\Phi 100 \text{ mm} \times 6 \text{ mm}$ was produced by combustion synthesis casting, and its compressive strength

reached 2200 MPa [94]. More alloys prepared by combustion synthesis casting and their properties can be found in Table 1.

Other than alloys, intermetallic compounds can be prepared by combustion synthesis casting in a high-pressure Ar atmosphere. La et al. prepared bulk nano-crystalline Fe_3Al intermetallic by combustion synthesis casting under an Ar pressure of 5 MPa [95]. The Fe_3Al sample showed a relative density of 98%, and consisted of roughly

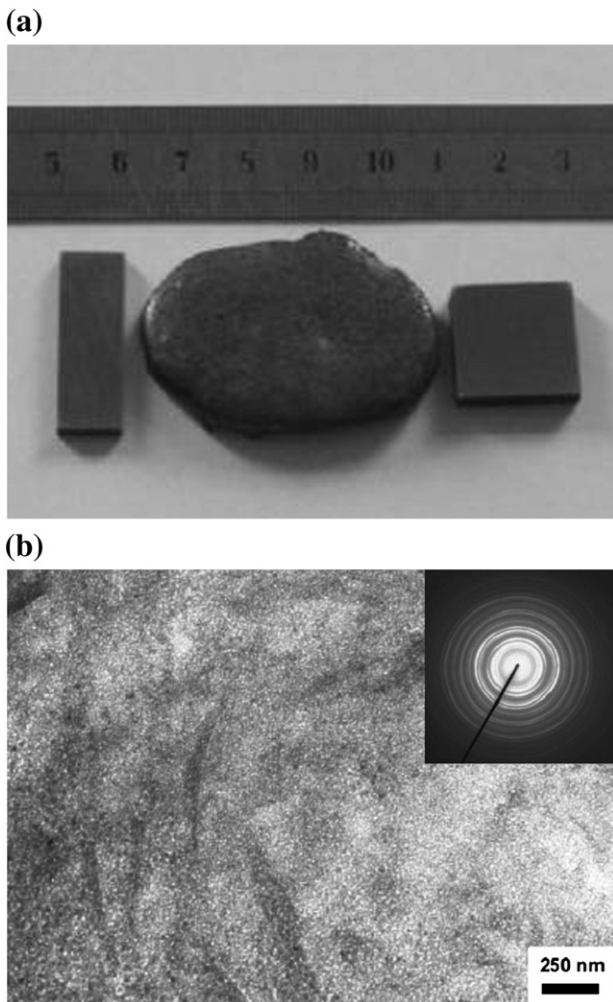


Fig. 9. Fe_3Al intermetallics prepared by combustion synthesis casting in an Ar atmosphere of 5 MPa: (a) photograph; (b) TEM image with SAED pattern [95].

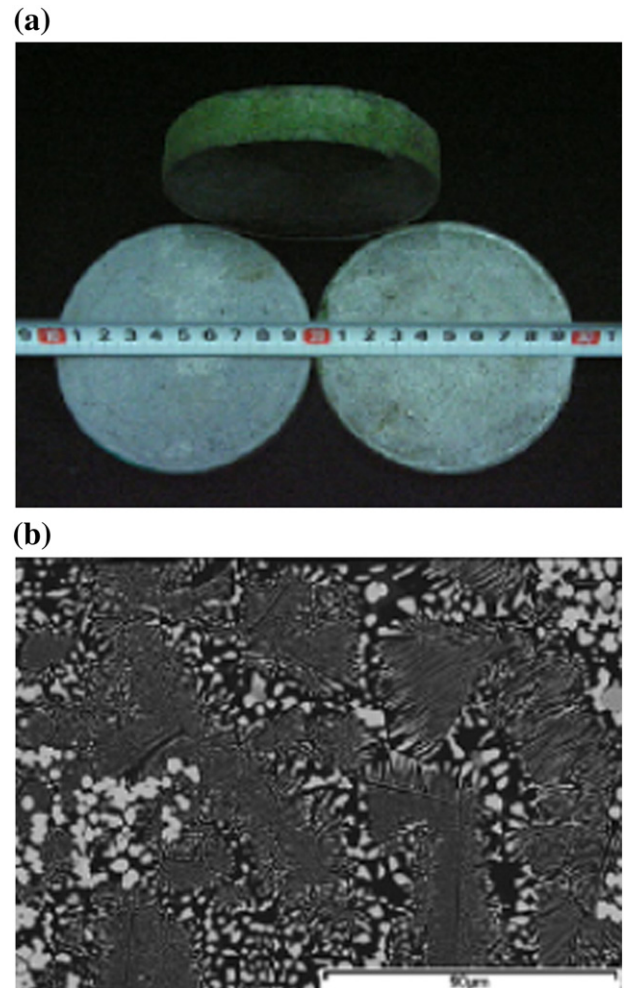


Fig. 10. $\text{Al}_2\text{O}_3/\text{ZrO}_2(\text{Y}_2\text{O}_3)$ eutectic ceramic composites prepared by high-gravity combustion synthesis: (a) photograph; (b) SEM image showing the eutectic microstructure [99].

equiaxial grains with a grain size of 10–25 nm (Fig. 9). The yield strength of the Fe_3Al sample was 1050 MPa and more than twice that of micro-crystalline Fe_3Al materials.

By combustion synthesis casting in a high-pressure Ar atmosphere, MoSi_2 – SiC composites were also fabricated [96]. In the composites, the grain morphology of SiC varied from particles to short fibers when its content was increased from 10 to 20 wt.%. In tribological tests, the composite with 20 wt.% SiC showed the best wear resistance.

As revealed by the above examples, a large variety of refractory and hard materials can be prepared by combustion synthesis casting in a high-pressure Ar atmosphere. This technique is especially useful for producing nanostructured alloys and intermetallics, whose large sample dimensions and improved mechanical properties reveal the great potential of the technique for practical applications.

4.2. Combustion synthesis casting in a high-gravity field

Compared with combustion synthesis casting of metals, combustion synthesis casting of ceramics is more difficult because most ceramic materials have extremely-high melting points (e.g. $\sim 2050^\circ\text{C}$ for Al_2O_3 , and $> 3000^\circ\text{C}$ for some carbides and borides). The high melting points result in a reduced lifetime and increased viscosity of ceramic melts, and make the removal of gas bubbles difficult. Consequently, most ceramic samples prepared by combustion synthesis casting showed a relatively high porosity and thus poor mechanical properties.

Recently, a new technique called high-gravity combustion synthesis was developed to carry out combustion synthesis casting in a high-gravity field [97–119]. The high-gravity field is induced by intensive centrifugation and introduced to accelerate the removal of gas bubbles from ceramic melts. By this technique, many refractory and hard materials have been prepared, such as ceramics [97–109], glasses [110–112],

glass-ceramics [113], alloys [114], intermetallics [115], and cermets [116,117].

High-gravity combustion synthesis was firstly used to produce multiphase ceramic composites. Zhao et al. prepared $\text{Al}_2\text{O}_3/\text{ZrO}_2(\text{Y}_2\text{O}_3)$ eutectic ceramic composites with the dimension of $\Phi 100\text{ mm} \times 20\text{ mm}$ (Fig. 10) by high-gravity combustion synthesis [99]. The relative density of the composites reached 99.8%. The composites were composed of randomly-orientated eutectic colonies containing orderly $t\text{-ZrO}_2$ fibers with a thickness ranging from submicron to nanometer scale. The eutectic ceramic composites showed excellent mechanical properties, where the hardness, flexural strength, and fracture toughness were 22.8 GPa, 1568 MPa, and $14.8\text{ MPa}\cdot\text{m}^{1/2}$, respectively. $\text{Al}_2\text{O}_3/\text{Y}_3\text{Al}_5\text{O}_{12}/\text{ZrO}_2$ ternary eutectic ceramics was also fabricated by high-gravity combustion synthesis [101], showing a relative density of 99.3%. The eutectic microstructure was characterized by an interpenetrating network of three phases with a submicron interphase spacing. The hardness and fracture toughness of the ternary eutectic ceramics were 17.82 GPa and $5.51\text{ MPa}\cdot\text{m}^{1/2}$.

Non-oxide TiC – TiB_2 ceramic composite was prepared by high-gravity combustion synthesis [103]. The relative density of the TiC – TiB_2 ceramic composite reached 99.2%. In the TiC – TiB_2 composite, fine TiB_2 platelets were embedded in the TiC matrix, and the boundary regions consisted of $(\text{Cr,Ti})\text{C}_{0.63}$ solid solution. The hardness, flexural strength, and fracture toughness of the TiC – TiB_2 composite were 28.5 GPa, $750 \pm 25\text{ MPa}$, and $6.2 \pm 0.5\text{ MPa}\cdot\text{m}^{1/2}$, respectively. Compared with the TiC – TiB_2 materials prepared by reactive sintering or hot-pressing, the TiC – TiB_2 composite produced by high-gravity combustion synthesis showed a higher hardness, which was attributed to the absence of intermediate borides and metallic binders and the formation of stable stoichiometric TiC phase.

Besides the multiphase ceramic composites, single-phase bulk ceramics were also fabricated by high-gravity combustion synthesis, such as Al_2O_3 , MgAl_2O_4 , and $\text{Y}_3\text{Al}_5\text{O}_{12}$ [105–108]. The density of the

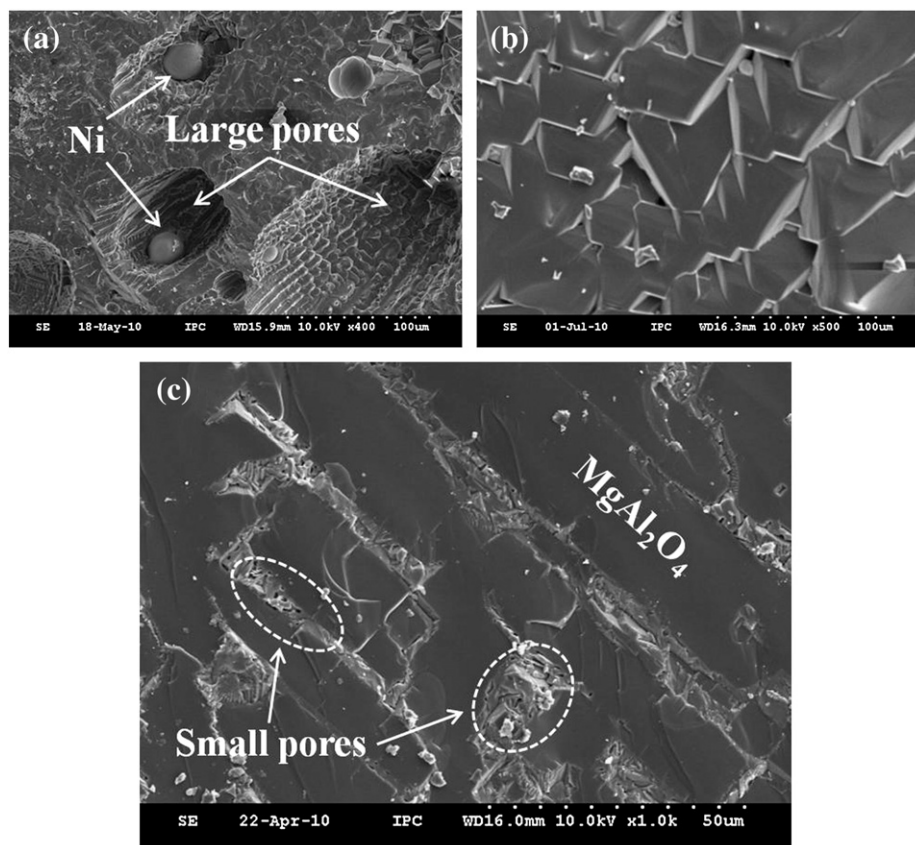


Fig. 11. SEM images of MgAl_2O_4 samples prepared by high-gravity combustion synthesis with different high-gravity factors: (a) $g'/g = 1$; (b) $g'/g = 200$; (c) $g'/g = 900$ [108].

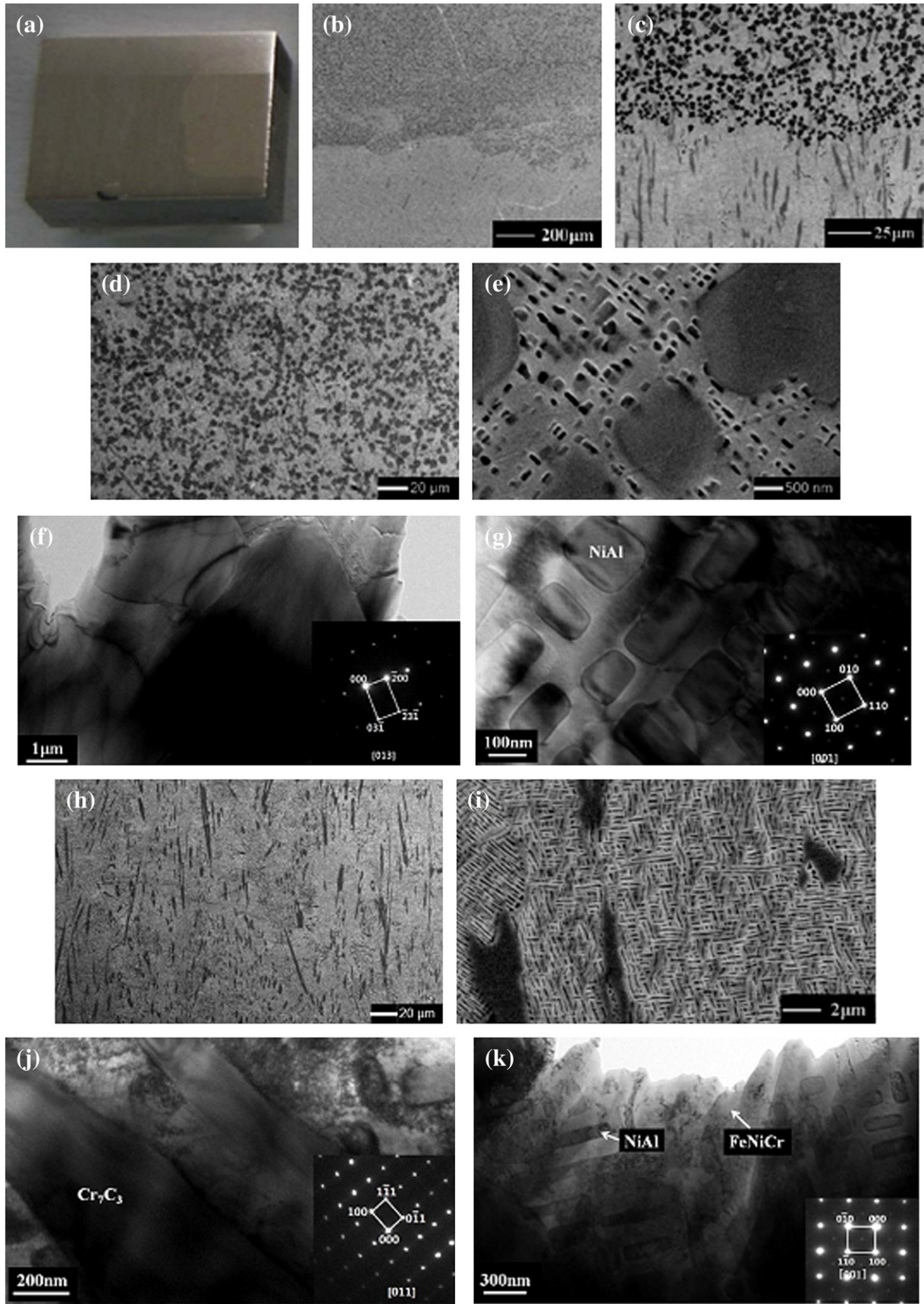


Fig. 12. FeNiCr/NiAl/TiC/Cr₇C₃ cermet prepared by high-gravity combustion synthesis: (a) photograph showing a double-layer structure; (b) and (c) SEM images of the interface between the two layers; (d) and (e) SEM images of the upper layer; (f) and (g) TEM images and SAED patterns of TiC and NiAl phases in the upper layer; (h) and (i) SEM images of the lower layer; (j) and (k) TEM images and SAED patterns of Cr₇C₃ and FeNiCr phases in the lower layer.

prepared ceramics increased with increasing high-gravity factors defined as g'/g , where g' was the acceleration in the high-gravity field and g means the conventional gravitational acceleration. Under a high-gravity factor of $g'/g=800$, the relative densities of the Al_2O_3 , MgAl_2O_4 , and $\text{Y}_3\text{Al}_5\text{O}_{12}$ ceramics were 93%, 92%, and 99%, respectively. With increasing high-gravity factors, both the porosity and pore size in the ceramics decreased (Fig. 11). The phase purity of the ceramic products also depended on the high-gravity factor. A larger high-gravity factor promoted the separation between metallic and ceramic melts, and led to a lower content of metallic impurities in the ceramics.

The application of high-gravity combustion synthesis was not limited to the fabrication of ceramics. It was also used for producing glasses, glass-ceramics, alloys, intermetallics, and cermets. For example, $\text{FeNiCr}/\text{NiAl}/\text{TiC}/\text{Cr}_7\text{C}_3$ cermets were prepared by high-gravity combustion synthesis [117]. The cermets showed a double-layer structure, as shown in Fig. 12. The upper layer was rich in TiC, with TiC grains of 1–4 μm evenly distributed in the FeNiCr matrix. Ultrafine NiAl crystallites with a size of 50–200 nm were precipitated in the FeNiCr matrix, and a coherent or semi-coherent orientation relationship between NiAl and FeNiCr was noticed. The lower layer consisted of a (FeNiCr + NiAl) matrix with an intertexture structure and acicular Cr_7C_3 grains embedded there. With a higher volume fraction of TiC, the upper layer showed a higher hardness (63 HRC) than that (54 HRC) of the lower layer. In tribological tests, the $\text{FeNiCr}/\text{NiAl}/\text{TiC}/\text{Cr}_7\text{C}_3$ cermets exhibited superior wear resistance to some commercial cemented carbides.

From the above results, combustion synthesis casting in a high-gravity field is a versatile technique for preparing a variety of refractory and hard materials, including ceramic materials with extremely-high melting points. In contrast to current methods (e.g. floating-zone, micro-pulling) for direct solidification of ceramics, high-gravity combustion synthesis requires no external heating sources and can be finished in a short time. For some single-phase ceramics prepared by high-gravity combustion synthesis, the purity and density should be further improved by preheating the reactants or applying a mechanical pressure, which will be well investigated in the future.

4.3. In-situ fabrication of metal matrix composites by incorporating combustion synthesis into conventional casting processes

In addition to the two techniques of combustion synthesis casting in a high-pressure Ar atmosphere or in a high-gravity field (as discussed in Sections 4.1 and 4.2), combustion synthesis can be incorporated into conventional casting processes to fabricate metal matrix composites. The principal idea of this method is to induce combustion reactions by the heat of molten metals during casting and realize in-situ synthesis of reinforcing ceramic phases. It is usually carried out by pouring the melt of the matrix metal (e.g. steel melt) onto preformed compacts of reactant powders for combustion synthesis. In this method, the metal melts are prepared by conventional furnace-melting, which is different from combustion synthesis casting. This method was firstly reported for preparing Mg-based metal matrix composites [120], and later used for producing steel matrix composites reinforced by ceramic particles [121–126].

Jiang et al. prepared steel-matrix composites reinforced with in-situ formed TiC particles by incorporating combustion synthesis into conventional casting [121]. The composites exhibited a microstructure with homogeneous distribution of TiC particles in the steel matrix. The hardness and wear resistance of the composites were enhanced by 67.6% and 349% compared with those of steel materials without ceramic reinforcing agents. Similarly, steel-matrix composites reinforced with $(\text{TiC} + \text{TiB}_2)$ particles were also fabricated [124,125]. The TiC and TiB_2 particles were in-situ synthesized by casting-induced combustion reaction of $(\text{Ni} + \text{Ti} + \text{CB}_4)$, and uniformly dispersed in the steel matrix. The porosity of the composites decreased with increasing Ni content, and almost fully-dense composites were obtained with 30 or 40 wt.% Ni. It was also found that, in the prepared composites the particle size of TiC

and TiB_2 depended on the starting CB_4 powders, and when finer CB_4 powder was used larger TiC and TiB_2 particles were produced. The hardness of the $(\text{TiC} + \text{TiB}_2)$ -reinforced steel-matrix composites was more than twice that of the un-reinforced steel materials.

By incorporating combustion synthesis into conventional casting processes, metal matrix composites reinforced with in-situ synthesized ceramic particles can be readily produced. The as-prepared steel-matrix composites showed much higher hardness than that of un-reinforced steel materials. In comparison with powder metallurgy, the casting approach exhibits several advantages to fabricate metal matrix composites, such as simplicity, flexibility, and availability for large-scale production. In this case, the incorporation of combustion synthesis into casting can provide a practical method for preparing metal matrix composites with improved hardness.

5. Concluding remarks

This article reviews recent progress in combustion synthesis of refractory and hard materials. In the last decade, a large diversity of refractory and hard materials has been prepared by combustion synthesis, including alloys, intermetallics, ceramics, and cermets. Combustion synthesis is not only available for producing ultrafine powders, but also can be used to fabricate consolidated bulk materials by combination with simultaneous densification or casting processes. The unique reaction condition in combustion synthesis, which is usually characterized by extremely-high temperature and fast heating/cooling rate, offers the products interesting microstructures (e.g. nano-crystallites, fine eutectic structure) and prominent mechanical properties (Table 1). Compared with conventional powder metallurgy approaches, combustion synthesis has the advantages of short processing time, less energy consumption, and lower cost, and thus can provide a more efficient way to produce refractory and hard materials.

In combustion synthesis of refractory and hard materials, investigations on reaction mechanisms are necessary for processing optimization to improve the properties of the products. In this aspect, many results were reported in the last decade, making a wide exploration of the reaction path, phase formation, microstructure evolution, and crystal growth in combustion synthesis [127–133]. Novel techniques such as in-situ time-resolved diffraction and infrared thermography were developed for real-time monitoring the samples during expeditious combustion reactions [134–136]. Computer simulation was also applied to study the combustion modes, reaction paths, and effect of processing parameters in combustion synthesis [137–139]. Such investigations can increase our knowledge on combustion synthesis of refractory and hard materials, and offer a guide for controlling the phase assemblage and microstructure of the products.

Acknowledgments

The authors gratefully acknowledge the financial support from National Natural Science Foundation of China (No. 50932006, 51002163), National Magnetic Confinement Fusion Science Program (No. 2010GB106000, 2010GB106003), and Beijing Natural Science Foundation (No. 2112043).

References

- [1] Merzhanov AG, Borovinskaya IP. Self-propagating high-temperature synthesis of refractory inorganic compounds. *Dokl Akad Nauk SSSR* 1972;204:366–9.
- [2] Munir ZA, Anselmi-Tamburini U. Self-propagating exothermic reactions: the synthesis of high-temperature materials by combustion. *Mater Sci Rep* 1989;3: 277–365.
- [3] Moore JJ, Feng HJ. Combustion synthesis of advanced materials. *Prog Mater Sci* 1995;39:243–316.
- [4] Makino A. Fundamental aspects of the heterogeneous flame in the self-propagating high-temperature synthesis process. *Prog Energy Combust Sci* 2001;27:1–74.

- [5] Filimonov IA, Kidin NI. High-temperature combustion synthesis: generation of electromagnetic radiation and the effect of external electromagnetic fields. *Combust Expl Shock Waves* 2005;41:639–56.
- [6] Mukasyan AS, White JDE. Combustion joining of refractory materials. *Int J SHS* 2007;16:154–68.
- [7] Mukasyan AS, Martirosyan KS, editors. *Combustion of Heterogeneous Systems: Fundamentals and Applications for Materials Synthesis*. Transworld Research Network; 2007.
- [8] Merzhanov AG, Borovinskaya IP. Historical retrospective of SHS: an autoreview. *Int J SHS* 2008;17:242–65.
- [9] McCauley JW, Puszynski JA. Historical perspective and contribution of US researchers into the field of self-propagating high-temperature synthesis (SHS)/combustion synthesis (CS): personal reflections. *Int J SHS* 2008;17:58–75.
- [10] Mukasyan AS, Rogachev AS. Discrete reaction waves: gasless combustion of solid powder mixtures. *Prog Energy Combust Sci* 2008;34:377–416.
- [11] Rogachev AS, Mukasyan AS. Combustion of heterogeneous nanostructural systems. *Combust Expl Shock Waves* 2010;46:243–66.
- [12] Lackner M, editor. *Combustion Synthesis: Novel Routes to Novel Materials*. Bentham Science Publishers; 2010.
- [13] Xanthopoulou G. Some advanced applications of SHS: an overview. *Int J SHS* 2011;20:269–72.
- [14] Levashov EA, Pogozhev YS, Kurbatkina VV. Advanced ceramic target materials produced by self-propagating high-temperature synthesis for deposition of functional nanostructured coatings. In: Sikaliadis C, editor. *Advances in ceramics: synthesis and characterization, processing and specific applications*. InTech; 2011. p. 3–48.
- [15] Liu GH, Li JT, Chen KX. Combustion synthesis of ceramic powders with controlled grain morphologies. In: Sikaliadis C, editor. *Advances in ceramics: synthesis and characterization, processing and specific applications*. InTech; 2011. p. 49–74.
- [16] Morsi K. The diversity of combustion synthesis processing: a review. *J Mater Sci* 2012;47:68–92.
- [17] Liu GH, Li JT, Chen KX. Review of melt-casting of bulk ceramics and glasses by high-gravity combustion synthesis. *Adv Appl Ceram* in press. <http://dx.doi.org/10.1179/174376712Y.0000000055>
- [18] Yeh CL, Chen YD. Combustion synthesis of vanadium carbonitride from V-C powder compacts under nitrogen pressure. *Ceram Int* 2007;33:365–71.
- [19] Liu GH, Li JT, Chen KX, Zhou HP. Combustion synthesis of (TiC + SiC) composite powders by coupling strong and weak exothermic reactions. *J Alloy Comp* 2010;492:82–6.
- [20] Yeh CL, Wang HJ. Combustion synthesis of vanadium borides. *J Alloy Comp* 2011;509:3257–61.
- [21] Liu GH, Chen KX, Zhou HP, Ning XS, Ferreira JMF. Effects of diluents and NH_4F additive on the combustion synthesis of Yb α -SiAlON. *J Eur Ceram Soc* 2005;25:3361–6.
- [22] Liu GH, Chen KX, Zhou HP, Jin HB, Pereira C, Agathopoulos S, et al. Tailoring of phase assemblage and grain morphology of (Nd, Dy)-containing SiAlON powders prepared by combustion synthesis. *Mater Sci Eng A* 2007;454–455:310–3.
- [23] Liu GH, Chen KX, Li JT. Combustion synthesis of SiAlON ceramic powders: A review. *Mater Manu Proc*, available on-line, <http://dx.doi.org/10.1080/10426914.2012.718471>.
- [24] Nersisyan HH, Won HI, Won CW, Lee JH. Study of the combustion synthesis process of nanostructured WC and WC-Co. *Mater Chem Phys* 2005;94:153–8.
- [25] Nersisyan HH, Won HI, Won CW. Combustion synthesis of WC powder in the presence of alkali salts. *Mater Lett* 2005;59:3950–4.
- [26] Won HI, Nersisyan HH, Won CW. Combustion synthesis of nano-sized tungsten carbide powder and effects of sodium halides. *J Nanopart Res* 2010;12:493–500.
- [27] Won HI, Nersisyan HH, Won CW, Lee JH. Simple synthesis of nano-sized refractory metal carbides by combustion process. *J Mater Sci* 2011;46:6000–6.
- [28] Nersisyan HH, Won HI, Won CW, Cho KC. Combustion synthesis of nanostructured tungsten and its morphological study. *Powder Technol* 2009;189:422–5.
- [29] Jiang GJ, Xu JY, Zhuang HR, Li WL. Fabrication of B_4C from $\text{Na}_2\text{B}_4\text{O}_7 + \text{Mg} + \text{C}$ by SHS method. *Ceram Int* 2011;37:1689–91.
- [30] Jiang GJ, Xu JY, Zhuang HR, Li WL. Fabrication of tungsten powder with sodium tungstate as raw material by SHS method. *Mater Lett* 2011;65:2969–71.
- [31] Mukasyan AS, Borovinskaya IP. Structure formation in SHS nitrides. *Int J SHS* 1992;1:55–63.
- [32] Borovinskaya IP, Barinova TV, Vershinnikov VI, Ignateva TI. SHS of ultrafine and nanosized refractory powders: an autoreview. *Int J SHS* 2010;19:114–9.
- [33] Borovinskaya IP, Ignateva TI, Semenova VN, Kovalev ID. SHS of ultrafine and nanosized MoSi_2 powders. *Int J SHS* 2011;20:113–7.
- [34] Liu GH, Yang K, Li JT, Du JS, Hou XY. Combustion synthesis of nanosized β -SiC powder on a large scale. *J Phys Chem C* 2008;112:6285–92.
- [35] Tsuchida T, Hasegawa T, Inagaki M. Self-combustion reactions induced by mechanical activation: formation of aluminum nitride from aluminum-graphite powder mixture. *J Am Ceram Soc* 1994;77:3227–31.
- [36] Shevchenko VG, Kononenko VI, Lukin NV, Latosh IN, Chupova IA. Effect of conditions under which powdered lanthanum is heated on its interaction with air. *Combust Expl Shock Waves* 1999;35:79–82.
- [37] Ilin AP, An VV, Vereshchagin VI, Yablunovskii GV. End combustion products of mixtures of ultrafine aluminum with a zirconium-aluminum alloy in air. *Combust Expl Shock Waves* 2000;36:209–12.
- [38] Gromov A, Vereshchagin V. Study of aluminum nitride formation by superfine aluminum powder combustion in air. *J Eur Ceram Soc* 2004;24:2879–84.
- [39] Liu GH, Chen KX, Zhou HP, Ren KG. Dynamically controlled formation of TiN by combustion of Ti in air. *J Am Ceram Soc* 2007;90:2918–25.
- [40] Mei L, Li JT. Synthesis of AlN–SiC solid solution through nitriding combustion of Al–C– Si_3N_4 in air. *Acta Mater* 2008;56:3543–9.
- [41] Li JT, Mei L, Yang Y, Lin ZM. Combustion synthesis of Si_3N_4 by selective reaction of silicon with nitrogen in air. *J Am Ceram Soc* 2009;92:636–40.
- [42] Liu GH, Chen KX, Zhou HP, Li JT, Pereira C, Ferreira JMF. Mechanical-activation-assisted combustion synthesis of α -SiAlON in normal air atmosphere. *Mater Res Bull* 2007;42:989–95.
- [43] Yang Y, Lin ZM, Li JT. Synthesis of SiC by silicon and carbon combustion in air. *J Eur Ceram Soc* 2009;29:175–80.
- [44] Liu GH, Li JT, Yang Y, Chen KX. Hollow spherical Ti–Al–C clusters prepared by combustion synthesis. *J Am Ceram Soc* 2009;92:2385–7.
- [45] Miyamoto Y, Koizumi M, Yamada O. High-pressure self-combustion sintering for ceramics. *J Am Ceram Soc* 1984;67:224–5.
- [46] Kunrath AO, Reimanis IE, Moore JJ. Microstructural evolution of titanium carbide–chromium carbide composites produced via combustion synthesis. *J Am Ceram Soc* 2002;85:1285–90.
- [47] Horvitz D, Gotman I. Pressure-assisted SHS synthesis of MgAl_2O_4 –TiAl in-situ composites with interpenetrating networks. *Acta Mater* 2002;50:1961–71.
- [48] Horvitz D, Gotman I, Gutmanas EY, Claussen N. In-situ processing of dense Al_2O_3 –Ti aluminide interpenetrating phase composites. *J Eur Ceram Soc* 2002;22:947–54.
- [49] Khoptiar Y, Gotman I. Synthesis of dense Ti_3SiC_2 -based ceramic by thermal explosion under pressure. *J Eur Ceram Soc* 2003;23:47–53.
- [50] Shon IJ, Munir ZA, Yamazaki K, Shoda K. Simultaneous synthesis and densification of MoSi_2 by field-activated combustion. *J Am Ceram Soc* 1996;79:1875–80.
- [51] Shon IJ, Kim HC, Rho DH, Munir ZA. Simultaneous synthesis and densification of Ti_5Si_3 and Ti_3Si_2 –20 vol% ZrO_2 composites by field-activated and pressure-assisted combustion. *Mater Sci Eng A* 1999;269:129–35.
- [52] Shon IJ, Rho DH, Kim HC, Munir ZA. Dense WSi_2 and WSi_2 –20 vol% ZrO_2 composite synthesized by pressure-assisted field activated combustion. *J Alloy Comp* 2001;322:120–6.
- [53] Lee JH, Jung JC, Won CW, Shon IJ. Simultaneous synthesis and densification of NiAl and Ni_3Al by pressure-assisted combustion. *J Mater Sci* 2002;37:2435–9.
- [54] Kim HC, Park CD, Jeong JW, Shon IJ. Synthesis of dense MoSi_2 by high-frequency induction heated combustion and its mechanical properties. *Met Mater Int* 2003;9:173–8.
- [55] Kim HC, Oh DY, Shon IJ. Synthesis of WC and dense WC–xvol% Co hard materials by high-frequency induction heated combustion method. *Int J Refract Metal Hard Mater* 2004;22:41–9.
- [56] Oh DY, Kim HC, Yoon JK, Shon IJ. One step synthesis of dense MoSi_2 –SiC composite by high-frequency induction heated combustion and its mechanical properties. *J Alloy Comp* 2005;395:174–80.
- [57] Kim HC, Shon IJ, Yoon JK, Lee SK, Munir ZA. One step synthesis and densification of ultra-fine WC by high-frequency induction combustion. *Int J Refract Metal Hard Mater* 2006;24:202–9.
- [58] Ko IY, Kim BR, Nam KS, Moon BM, Lee BS, Shon IJ. Pulsed current activated combustion synthesis and consolidation of ultrafine NbSi_2 from mechanically activated powders. *Met Mater Int* 2009;15:399–403.
- [59] Shon IJ, Park JH, Yoon JK, Park HK. Consolidation of nanostructured ZrSi_2 – Si_3N_4 synthesized from mechanically activated (4ZrN + 11Si) powders by high frequency induction heated combustion synthesis. *Mater Res Bull* 2009;44:1462–7.
- [60] Ko IY, Park JH, Nam KS, Shon IJ. Rapid consolidation of nanocrystalline NbSi_2 – Si_3N_4 composites by pulsed current activated combustion synthesis. *Met Mater Int* 2010;16:393–8.
- [61] Ko IY, Bae SK, Yoon JK, Shon IJ. Rapid synthesis and consolidation of nanostructured TaSi_2 –SiC– Si_3N_4 composite from mechanically activated powders by high-frequency induction-heated combustion. *J Alloy Comp* 2010;504:548–51.
- [62] Ko IY, Park JH, Yoon JK, Nam KS, Shon IJ. ZrSi_2 –SiC composite obtained from mechanically activated $\text{ZrC} + 3\text{Si}$ powders by pulsed current activated combustion synthesis. *Ceram Int* 2010;36:817–20.
- [63] Shon IJ, Park JH, Ko IY, Doh JM, Yoon JK, Nam KS. Properties and consolidation of nanocrystalline WSi_2 –SiC composite from mechanically activated powders by pulsed current activated combustion synthesis. *Ceram Int* 2011;37:1549–55.
- [64] Zhang XH, Zhu CC, Qu W, He XD, Kvanin VL. Self-propagating high temperature combustion synthesis of TiC/TiB₂ ceramic-matrix composites. *Compos Sci Technol* 2002;62:2037–41.
- [65] Zhang XH, He XD, Han JC, Qu W, Kvanin VL. Combustion synthesis and densification of large-scale TiC–xNi cermets. *Mater Lett* 2002;56:183–7.
- [66] Zhang WF, Zhang XH, Wang JL, Hong CQ. Effect of Fe on the phases and microstructure of TiC–Fe cermets by combustion synthesis/quasi-isostatic pressing. *Mater Sci Eng A* 2004;381:92–7.
- [67] Zhang XH, Xu Q, Han JC, Kvanin VL. Self-propagating high temperature combustion synthesis of TiB/Ti composites. *Mater Sci Eng A* 2003;348:41–6.
- [68] Xu Q, Zhang XH, Han JC, He XD, Kvanin VL. Combustion synthesis and densification of titanium diboride–copper matrix composite. *Mater Lett* 2003;57:4439–44.
- [69] Zhang XH, Yan C, Yu ZZ. In-situ combustion synthesis of ultrafine TiB₂ particles reinforced Cu matrix composite. *J Mater Sci* 2004;39:4683–5.
- [70] Wang LJ, Jiang W, Qin C, Chen LD. Effect of starting SiC particle size on in situ fabrication of Ti_5Si_3 /TiC composites. *Mater Sci Eng A* 2006;425:219–24.
- [71] Zhang JF, Wang LJ, Shi L, Jiang W, Chen LD. Rapid fabrication of Ti_3SiC_2 –SiC nanocomposite using the spark plasma sintering-reactive synthesis method. *Scr Mater* 2007;56:241–4.
- [72] Zhao Y, Wang LJ, Zhang GJ, Jiang W, Chen LD. Preparation and microstructure of a ZrB_2 –SiC composite fabricated by the spark plasma sintering-reactive synthesis method. *J Am Ceram Soc* 2007;90:4040–2.
- [73] Zhao Y, Wang LJ, Zhang GJ, Jiang W, Chen LD. Effect of holding time and pressure on properties of ZrB_2 –SiC composite fabricated by the spark plasma sintering reactive synthesis method. *Int J Refract Metal Hard Mater* 2009;227:177–80.
- [74] Morsi K, Moussa O, Wall JJ. Simultaneous combustion synthesis (thermal explosion mode) and extrusion of nickel aluminides. *J Mater Sci* 2005;40:1027–30.

- [75] Morsi K, Goyal S. Equal channel angular pressing followed by combustion synthesis of titanium aluminides. *J Alloy Comp* 2007;429:1–4.
- [76] Shu SL, Lu JB, Qiu F, Xuan QQ, Jiang QC. Effects of alloy elements (Mg, Zn, Sn) on the microstructures and compression properties of high-volume-fraction TiC_x/Al composites. *Scr Mater* 2010;63:1209–11.
- [77] Shu SL, Lu JB, Qiu F, Xuan QQ, Jiang QC. High volume fraction TiC_x/Al composites with good comprehensive performance fabricated by combustion synthesis and hot press consolidation. *Mater Sci Eng A* 2011;528:1931–6.
- [78] Shu SL, Qiu F, Jin SB, Lu JB, Jiang QC. Compression properties and work-hardening behavior of Ti₂AlC/TiAl composites fabricated by combustion synthesis and hot press consolidation in the Ti–Al–Nb–C system. *Mater Des* 2011;32:5061–5.
- [79] Zhao HL, Qiu F, Jin SB, Jiang QC. High room-temperature plastic and work-hardening effect of the NiAl-matrix composites reinforced by particulates. *Intermetallics* 2011;19:376–81.
- [80] Shibuya M, Ohyanagi M, Munir ZA. Simultaneous synthesis and densification of titanium nitride/titanium diboride composites by high nitrogen pressure combustion. *J Am Ceram Soc* 2002;85:2965–70.
- [81] Smirnov KL, Borovinskaya IP. Combustion synthesis of SiAlON-based ceramic composites. *Powder Metall Met Ceram* 2003;42:11–2.
- [82] Zhao YS, Yang Y, Li JT, Borovinskaya IP, Smirnov KL. Combustion synthesis and tribological properties of SiAlON-based ceramic composites. *Int J SHS* 2010;19:172–7.
- [83] Li HB, Zheng YT, Han JC, Zhou LJ. Microstructure, mechanical properties and thermal shock behavior of h-BN–AlN ceramic composites prepared by combustion synthesis. *J Alloy Comp* 2011;509:1661–4.
- [84] Li HB, Zheng YT, Han JC, Zhou LJ. Effect of reactant Ti/B4C ratio on the stoichiometry and mechanical properties of h-BN–Ti(C, N) prepared by combustion synthesis. *Mater Sci Eng A* 2011;528:2380–4.
- [85] Yang J, La PQ, Liu WM, Hao Y. Microstructure and properties of Fe₃Al–Fe₃AlC_{0.5} composites prepared by self-propagating high temperature synthesis casting. *Mater Sci Eng A* 2004;382:8–14.
- [86] Yang J, Ma JQ, Liu WM, Bi QL, Xue QJ. Large-scale Fe–C nanoeutectic alloy prepared by a self-propagating high-temperature synthesis casting route. *Scr Mater* 2008;58:1074–7.
- [87] Fu LC, Yang J, Bi QL, Zhu SY, Liu WM. Dry-sliding tribological properties of nano-eutectic Fe₈₃B₁₇ alloy. *Tribol Lett* 2009;34:185–91.
- [88] Fu LC, Yang J, Bi QL, Liu WM. Nanostructured hypoeutectic Fe–B alloy prepared by a self-propagating high temperature synthesis combining a rapid cooling technique. *Nanoscale Res Lett* 2009;4:11–6.
- [89] Fu LC, Yang J, Bi QL, Liu WM. Enhanced ductility of dendrite-ultrafine eutectic composite Fe₃B alloy prepared by a self-propagating high-temperature synthesis. *Adv Eng Mater* 2009;11:194–7.
- [90] Fu LC, Yang J, Bi QL, Liu WM. Pressure-assisted combustion synthesis large-scale nanostructured Fe₇₄Si₂₄B₂ alloy. *Physica B* 2010;405:4497–9.
- [91] Li LJ, Yang J, Bi QL, Ma JQ, Liu WM. Combustion synthesis and characterization of bulk nanocrystalline Fe₈₈Si₁₂ alloy. *IEEE Trans Nanotechnol* 2010;9:218–22.
- [92] Fu LC, Yang J, Bi QL, Liu WM. Microstructure and mechanical behaviour of (Fe₈₈Si₁₂)₉₅Al₅ alloy prepared by aluminothermics. *Mater Sci Technol* 2011;27:1482–4.
- [93] Fu LC, Yang J, Bi QL, Liu WM. Microstructure and mechanical behavior of nano-structured composite Cu₆₀Fe₄₀ alloy. *Phil Mag Lett* 2011;91:78–85.
- [94] Ma JQ, Yang J, Bi QL, Fu LC, Kang YH, Liu WM. Combustion synthesis of large bulk nanostructured Ni₆₅Al₂₁Cr₁₄ alloy. *J Nanomater* 2011;934801.
- [95] La P, Yang J, Cockayne DJH, Liu WM, Xue Q, Li Y. Bulk nanocrystalline Fe₃Al-based material prepared by aluminothermic reaction. *Adv Mater* 2006;18:733–7.
- [96] La P, Xue QJ, Liu WM. Study of wear resistant MoSi₂–SiC composites fabricated by self-propagating high temperature synthesis casting. *Intermetallics* 2003;11:541–50.
- [97] Zhao ZM, Zhang L, Zheng H, Bai HB, Zhang SY, Xu BC. Microstructures and mechanical properties of Al₂O₃/ZrO₂ composite produced by combustion synthesis. *Scr Mater* 2005;53:995–1000.
- [98] Zhao ZM, Zhang L, Song YG, Wang WG, Wu J. Microstructures and properties of rapidly solidified Y₂O₃ doped Al₂O₃/ZrO₂ composites prepared by combustion synthesis. *Scr Mater* 2006;55:819–22.
- [99] Zhao ZM, Zhang L, Song YG, Wang WG. Al₂O₃/ZrO₂ (Y₂O₃) self-growing composites prepared by combustion synthesis under high gravity. *Scr Mater* 2008;58:207–10.
- [100] Mei L, Mai PL, Li JT, Chen KX. Fabrication of nanostructure Al₂O₃/ZrO₂(Y₂O₃) eutectic by combustion synthesis melt-casting under ultra-high gravity. *Mater Lett* 2010;64:68–70.
- [101] Liang R, Pei J, Li JT, Chen KX. Fabrication of Al₂O₃/YAG/ZrO₂ ternary eutectic by combustion synthesis melt-casting under ultra-high gravity. *J Am Ceram Soc* 2009;92:549–52.
- [102] Su GL, Zhao ZM, Zhang L, Huang XG, Pan CZ. Large-bulk solidified Al₂O₃–ZrO₂–Y₂O₃ prepared by self-pressure assisting combustion synthesis under high gravity. *Adv Mater Res* 2011;177:394–7.
- [103] Zhao ZM, Zhang L, Song YG, Wang WG, Liu HB. Microstructures and properties of large bulk solidified TiC–TiB₂ composites prepared by combustion synthesis under high gravity. *Scr Mater* 2009;61:281–4.
- [104] Huang XG, Zhang L, Zhao ZM, Pan CZ, Su GL. TiB₂–(Ti, W)C eutectic composite ceramics prepared by combustion synthesis under high gravity. *Adv Mater Res* 2011;177:386–9.
- [105] Pei J, Li JT, Liu GH, Chen KX. Fabrication of bulk Al₂O₃ by combustion synthesis melt-casting under ultra-high gravity. *J Alloy Comp* 2009;476:854–8.
- [106] Song YP, Kim HS, Lee CS, Li JT, Pei J. Predicting the adiabatic temperature of transparent Y₃Al₅O₁₂ prepared via combustion synthesis under ultra-high gravity. *Mater Trans* 2010;51:2230–5.
- [107] Liu GH, Li JT, Guo SB, Ning XS, Chen YX. Melt-casting of YAG ceramics by combustion synthesis under high gravity with the addition of glass. *J Alloy Comp* 2011;509:213–5.
- [108] Liu GH, Li JT, Yang ZC. Melt-casting of translucent MgAl₂O₄ ceramics by combustion synthesis under high gravity. *Mater Manu Proc* 2012;27:689–93.
- [109] Liu GH, Li J, Yang ZC. Preparing bulk ceramics by high-gravity combustion synthesis. *Key Eng Mater* 2012;512–515:350–3.
- [110] Liu GH, Li JT, He B. Melt-casting of Si–Al–Y–O glasses and glass-ceramics by combustion synthesis under high gravity. *J Non-Cryst Solids* 2011;357:1764–7.
- [111] He B, Liu GH, Li JT, Wu L, Yang ZC, Guo SB, et al. Preparation of Y₂O₃–Al₂O₃–SiO₂ glasses by combustion synthesis melt-casting under high gravity. *Mater Res Bull* 2011;46:1035–8.
- [112] Yang ZC, Liu GH, Li JT, Guo SB, Xu LH. Preparation of transparent Y₂O₃–Al₂O₃–SiO₂ glasses by high-gravity combustion synthesis with heating assistance. *J Am Ceram Soc* 2012;95:1799–802.
- [113] Liu GH, Li JT, He B. Fast fabrication of glass-ceramics by high-gravity combustion synthesis. *Adv Appl Ceram* 2011;110:394–9.
- [114] Mai PL, Fang WL, Liu GH, Chen YX, He SL, Li JT. Preparation of W–Ni graded alloy by combustion synthesis melt-casting under ultra-high gravity. *Mater Lett* 2011;65:3496–8.
- [115] Mai PL, Liu GH, He SL, Li JT. Preparation of Fe₃Al intermetallics by combustion synthesis melt-casting under ultra-high gravity. *Mater Manu Proc* 2012;27:486–9.
- [116] Liu GH, Li JT, Chen KX. Combustion synthesis of porous TiC/Ni composites under high gravity. *Adv Appl Ceram* 2012;111:404–7.
- [117] Xu TG, Xi WJ, Guo SB, Liu GH, Li JT. Thermite synthesis of TiC/FeNiCr cermet with double-layer structure. submitted for publication.
- [118] Liu GH, Li JT, Chen KX, Chen YX, Jiang ZJ, Song YP. Microstructure evolution of ceramic materials during solidification from melts in high-gravity combustion synthesis. *Mater Res Bull* 2012;47:222–34.
- [119] Liu GH, Li JT, Chen YX. Phase separation in melt-casting of ceramic materials by high-gravity combustion synthesis. *Mater Chem Phys* 2012;133:661–7.
- [120] Jiang QC, Li XL, Wang HY. Fabrication of TiC particulate reinforced magnesium matrix composites. *Scr Mater* 2003;48:713–7.
- [121] Jiang QC, Zhao F, Wang HY, Zhang ZQ. In-situ TiC-reinforced steel composite fabricated via self-propagating high-temperature synthesis of Ni–Ti–C system. *Mater Lett* 2005;59:2043–7.
- [122] Wang HY, Jiang QC, Ma BX, Wang Y, Zhao F. Fabrication of steel matrix composites locally reinforced with in situ TiB₂ particulates using self-propagating high-temperature synthesis reaction of Ni–Ti–B system during casting. *Adv Eng Mater* 2005;7:58–63.
- [123] Jiang QC, Ma BX, Wang HY, Wang Y, Dong YP. Fabrication of steel matrix composites locally reinforced with in situ TiB₂–TiC particulates using self-propagating high-temperature synthesis reaction of Al–Ti–B₄C system during casting. *Composites Part A* 2006;37:133–8.
- [124] Yang YF, Wang HY, Zhao RY, Liang YH, Jiang QC. Fabrication of steel matrix composites locally reinforced with different ratios of TiC/TiB₂ particulates using SHS reactions of Ni–Ti–B₄C and Ni–Ti–B₄C–C systems during casting. *Mater Sci Eng A* 2007;445–446:398–404.
- [125] Yang YF, Wang HY, Zhao RY, Liang YH, Jiang QC. In situ TiC/TiB₂ particulate locally reinforced steel matrix composites fabricated via the SHS reaction of Ni–Ti–B₄C system. *Int J Appl Ceram Technol* 2009;6:437–46.
- [126] Zou BL, Shen Ping, Cao XQ, Jiang QC. The mechanism of thermal explosion (TE) synthesis of TiC–TiB₂ particulate locally reinforced steel matrix composites from an Al–Ti–B₄C system via a TE-casting route. *Mater Chem Phys* 2012;132:51–62.
- [127] Biswas A, Roy SK. Comparison between the microstructural evolutions of two modes of SHS of NiAl: key to a common reaction mechanism. *Acta Mater* 2004;52:257–70.
- [128] Biswas A. Porous NiTi by thermal explosion mode of SHS: processing, mechanism, and generation of single phase microstructure. *Acta Mater* 2005;53:1415–25.
- [129] Liu GH, Chen KX, Tian JJ, Zhou HP, Pereira C, Ferreira J. Fast shape evolution of TiN micro-crystals in combustion synthesis. *Cryst Growth Des* 2006;6:2404–11.
- [130] Liu GH, Chen KX, Zhou HP, Guo JM, Ren KG, Ferreira JMF. Layered growth of Ti₂AlC and Ti₃AlC₂ in combustion synthesis. *Mater Lett* 2007;61:779–84.
- [131] Liu GH, Chen KX, Li JT. Growth mechanism of crystalline SiAlON microtubes prepared by combustion synthesis. *CrystEngComm* 2012;14:5585–8.
- [132] Khoshkhoo MS, Shamanian M, Saidi A, Abbasi MH, Panjehpour M, Javid FA. The effect of Mo particle size on SHS synthesis mechanism of MoSi₂. *J Alloy Comp* 2009;475:529–34.
- [133] Zou BL, Shen P, Cao XQ, Jiang QC. Reaction path of the synthesis of α-Al₂O₃–TiC–TiB₂ in an Al–TiO₂–B₄C system. *Int J Refract Metal Hard Mater* 2011;29:591–5.
- [134] Contreras L, Turrillas X, Vaughan GBM, Kvick A, Rodriguez MA. Time-resolved XRD study of TiC–TiB₂ composites obtained by SHS. *Acta Mater* 2004;52:4783–90.
- [135] Carole D, Frety N, Paris S, Vrel D, Bernard F, Marin-Ayral RM. Investigation of the SHS mechanisms of titanium nitride by in situ time-resolved diffraction and infrared thermography. *J Alloy Comp* 2007;436:181–6.
- [136] Mas-Guindal MJ, Turrillas X, Hansen T, Rodriguez MA. Time-resolved neutron diffraction study of Ti–TiC–Al₂O₃ composites obtained by SHS. *J Eur Ceram Soc* 2008;28:2975–82.
- [137] Gennari S, Maglia F, Anselmi-Tamburini U, Spinolo G. Combustion modes and reaction paths of the self-sustained high-temperature Synthesis of intermetallic compounds: a computer simulation study of the effect of exothermicity. *J Phys Chem B* 2004;108:19550–6.
- [138] Gennari S, Anselmi-Tamburini U, Maglia F, Spinolo G, Munir ZA. A new approach to the modeling of SHS reactions: combustion synthesis of transition metal aluminides. *Acta Mater* 2006;54:2343–51.
- [139] Gennari S, Anselmi-Tamburini U, Maglia F, Spinolo G. Modeling the ignition of self-propagating combustion synthesis of transition metal aluminides. *Intermetallics* 2010;18:2385–93.